Computers in Industry 177 (2026) 104449



Contents lists available at ScienceDirect

Computers in Industry

journal homepage: www.sciencedirect.com/journal/computers-in-industry





Advancing process monitoring: A distribution-free control framework for operation processes

Zsolt T. Kosztyán [a,e,f,*], Andrew MacClever [a], Zahid Khan [a], Csaba Hegedűs [b], Aamir Saghir [c], Tibor Csizmadia [d], Attila I. Katona [a]

[a] Department of Quantitative Methods, University of Pannonia, Egyetem str. 10., Veszprém, Hungary
[b] Department of Supply Chain Management, University of Pannonia, Egyetem utca 10., Veszprém, Hungary
[c] Department of Statistics, Mirpur University of Sciences and Technology, Mirpur-10250, Pakistan
[d] Institute of Management, Faculty of Business and Economics, University of Pannonia, Egyetem street 10., Veszprém, Hungary
[e] Institute of Institute of Advanced Studies, Kőszeg (iASK), Chernel street 14., Kőszeg, Hungary
[f] Wekerle International University, Jázmin street 14., Kőszeg, Hungary

ARTICLE INFO

Keywords:
Operation process
Statistical control charts
Distribution independence

ABSTRACT

Statistical process control and control charts are essential tools for monitoring and controlling production processes across various sectors, including healthcare, finance, software development, and education. Despite the prevalence of operation processes (OPs) in all economic fields, there is no dedicated control chart to monitor them. This paper presents a new OP control chart and its associated fitting procedure. The proposed method is illustrated using a real-life OP. The performance of the control chart is also investigated under nonnormality, and several distribution-free chart statistics are compared to identify the most effective design. Practical recommendations are provided to guide decision makers in selecting appropriate control charts for OPs.

1. Introduction

Statistical process control (SPC) comprises tools widely applied in the manufacturing and production industries to monitor and control process quality (Almazah et al., 2021). Among the most prominent SPC tools are control charts, which graphically represent process data over time and help detect deviations from expected performance or signs that the process is no longer under control.

The use of control charts can provide several benefits for organizations, such as improved quality, reduced waste, increased manufacturing efficiency, and reduced costs (Khorshidi et al., 2016). Control charts also help organizations identify and correct problems in the production process before they lead to defective products or services.

Despite their benefits, applying control charts poses challenges, including selecting appropriate chart types (Waqas et al., 2023, 2025; Williams and Ziemnik, 2025), setting appropriate control limits (Kosztyán and Katona, 2016; Qiu et al., 2020; Knoth, 2021), determining the appropriate sample size and frequency (Kosztyán and Katona, 2018), and correctly interpreting the data. Organizations must also ensure that employees are trained in the proper use of control charts and that they understand the importance of maintaining process control.

Several types of control charts are available, including the most commonly used X-bar and R charts (for sample means and sample ranges), X-bar and S charts (for sample means and standard deviations), p-charts (for reject ratio), and c-charts (for number of defects or nonconformities) (Oakland and Oakland, 2018). Each chart type is used to monitor a specific type of process data, such as the mean and variability of a process or the proportion of nonconforming items in a sample.

Although X-bar, R, and S charts are widely used, they have notable limitations. For example, their accuracy significantly depends on the *sample size* (Hillier, 1967). If the sample size is too small, the monitoring scheme may not accurately reflect process variability, leading to incorrect decisions. *Normality assumption* (Schilling and Nelson, 1976): The X-bar, R, and S charts assume that the data follow a normal distribution. If the data are not normally distributed, the chart may not accurately reflect process variability, leading to incorrect decisions (Albers et al., 2004; Li et al., 2018). *Out-of-control conditions* (Klein, 2000; Kostyszyn et al., 2021): X-bar, R, and S charts are designed to detect shifts in the process mean and variability. However, they may not detect other types of out-of-control patterns, such as cycles, trends, and mixtures. *Inability*

* Corresponding author.
E-mail addresses: kosztyan.zsolt@gtk.uni-pannon.hu (Z.T. Kosztyán), macclever.andrew@gtk.uni-pannon.hu (A. MacClever), zainkhan@hu.edu.pk (Z. Khan), hegedus.csaba@gtk.uni-pannon.hu (C. Hegedűs), aamirstat@yahoo.com (A. Saghir), csizmadia.tibor@gtk.uni-pannon.hu (T. Csizmadia), katona.attila@gtk.uni-pannon.hu (A.I. Katona).

https://doi.org/10.1016/j.compind.2026.104449
Received 31 July 2024; Received in revised form 18 October 2025; Accepted 12 February 2026
Available online 20 February 2026
0166-3615/© 2026 The Authors. Published by Elsevier B.V. This is an open access article under the CC BY license (http://creativecommons.org/licenses/by/4.0/).

to pinpoint specific causes (Koutras et al., 2007; Ruiz-Tamayo et al., 2021): X-bar, R, and S charts do not provide information on the specific causes of process variation. Additional tools, such as Pareto charts or cause-and-effect diagrams, may be needed to identify the root cause of a problem. *Difficulty in setting appropriate control limits* (Chakraborti et al., 2001; Katona, 2022): Setting appropriate control limits can be challenging, particularly for processes with high variability or small sample sizes. If the control limits are too wide or too narrow, the chart may not accurately reflect process variability, leading to incorrect decisions. *Limitations in detecting small shifts* (Davis and Woodall, 1988; Mastrangelo and Brown, 2000; Zhou et al., 2020): X-bar, R, and S charts may not be sensitive enough to detect small shifts in process mean or variability. In these cases, more sensitive charts, such as the exponentially weighted moving average (EWMA) control chart or cumulative sum (CUSUM) chart, may be needed.It is important to consider the above limitations when using X-bar, R, and S charts and to employ other tools and techniques as needed to supplement the information provided by these charts. Distribution-free control charts (Bakir, 2004; Xue et al., 2024; Diaz Pulido et al., 2025; Chen et al., 2025), also known as distribution-independent or nonparametric control charts, are designed to address some of the limitations of traditional control charts, including X-bar, R, and S charts. Distribution-free control charts can overcome the limitations of traditional control charts in several ways: (1) Nonparametric control charts are unaffected by the underlying distribution of the data. Therefore, they do not require the assumption of normality, which is a limitation of traditional control charts. (2) These charts are robust even with small sample sizes, making them useful for processes with limited data. (3) They can detect a wide range of out-of-control conditions, including shifts, trends, cycles, mixtures, and outliers, making them more sensitive than traditional control charts are. (4) They are useful for recognizing the presence of specific cause variations, making it easier to identify the root causes of process problems. (5) Distribution-free control charts are easy to use and interpret, making them practical tools for process improvement.

Several examples of distribution-free control charts include the median chart (Castagliola and Figueiredo, 2013), the median absolute deviation (MAD) chart (Adekeye et al., 2021), the sign chart (Wu et al., 2002; Abbas et al., 2021), and the distribution-free Shewhart chart (Bakir, 2004). These charts are typically used in industries such as healthcare, finance, and manufacturing. Overall, distribution-free control charts provide a useful alternative to traditional control charts, particularly in cases with nonnormal data or a limited sample size.

Median, range, or sign tests do not require data to follow a specific distribution, making distribution-free control charts more robust and suitable for monitoring processes with nonnormal data (Chakraborti and Graham, 2019); they may be less sensitive than traditional univariate control charts in detecting small process changes, particularly if the process is normally distributed (Perdikis et al., 2024).

Overall, the choice between distribution-free and traditional univariate control charts depends on the nature of the process being monitored, the data being collected, and the specific goals of the quality control program. Although distribution-free control charts are more flexible and robust than traditional univariate control charts are, they still have assumptions and limitations that should be considered when they are used. Like traditional univariate control charts, nonparametric control charts assume that the data are independent and identically distributed (i.i.d.). Violations of this assumption, such as autocorrelation and heteroskedasticity, can affect the validity of the control chart.

Most nonparametric control charts are designed primarily to detect shifts in process location; however, monitoring process variability is equally important. Several nonparametric control charts are available for tracking process variability. An excellent overview of this topic for univariate and multivariate processes can be found in the literature (Qiu and Li, 2011; Chakraborti and Graham, 2019; Li et al., 2020; Ahmed et al., 2024; Abbas et al., 2024). Furthermore, notable studies have focused on the joint monitoring of location and variability, such as the control charts developed by Zhou et al. (2010), Mukherjee and Chakraborti (2012), Chowdhury et al. (2014) and Diaz Pulido et al. (2023) or Alevizakos et al. (2024).

The median charts use the median of the process data to monitor the process over time. The median is less sensitive to extreme values and outliers than the mean is, making it a useful statistic for nonnormal data (Graham et al., 2010; Castagliola et al., 2013; Tran et al., 2019). Note that the median chart also belongs to the Shewhart control chart family (see ISO Central Secretary, 2023). As another solution, range charts use the range (i.e., the difference between the maximum and minimum values) of process data to monitor process variability over time. Range charts are useful for detecting shifts in process dispersion, regardless of the underlying distribution (Mukherjee and Chakraborti, 2012; Abbas et al., 2023; Wang et al., 2024). Sign charts use the signs of the differences between consecutive process measurements to monitor a process over time (Godase and Mahadik, 2024). Sign charts are often used for binary data or data that can be converted to binary form (Bakir, 2004; Yang et al., 2011). The Wilcoxon–Mann–Whitney test uses the Wilcoxon rank sum test or Mann–Whitney U test to compare the process data to a reference value (Abid et al., 2017). These tests are nonparametric and can detect location changes, regardless of the underlying distribution (Jayathavaj and Pongpullponsak, 2014; Mukherjee and Sen, 2015; Sabahno and Amiri, 2023). Run charts use the frequency of runs (i.e., consecutive data points with the same sign or value) to monitor a process over time. Run charts can be used for binary and nonbinary data (Castagliola et al., 2013; Teoh et al., 2017; Li et al., 2020)

SPC can be used in many different areas beyond production processes: *healthcare* (Thor et al., 2007; Ahmadini et al., 2025), where SPC is used to monitor and improve healthcare processes, such as patient wait times, medication errors, and infection rates; *finance* (Severin and Schmid, 1998), where SPC monitors financial processes, such as transaction processing times, account reconciliation, and fraud detection; *software development* (Caivano, 2005), where SPC controls software development processes, such as code review times, bug fix rates, and testing effectiveness; *customer service* (Kim and Lim, 2021; Shi et al., 2025), where SPC improves customer service processes, such as call center wait times, response times for customer inquiries, and customer satisfaction rates; *supply chain management* (Hajej et al., 2021; Zhong and Jia, 2025), where SPC monitors supply chain processes, such as order processing times, inventory levels, and shipping accuracy; *education* (Bi, 2022), where SPC can be used to monitor and improve student performance, teacher effectiveness, and classroom processes; and *project management* (Colin and Vanhoucke, 2015; Toma et al., 2025), where SPC controls the makespan and the project cost to maintain deadlines and project budgets. Nevertheless, to our knowledge, no study exists in which SPC is used in operations or operation processs (OPs). We define OPs in accordance with Scheer et al. (2006); they include processes such as sequences of connected tasks that produce value on the basis of the needs of business partners. Despite the many differences between technology or manufacturing processes and OPs, we believe that SPC logic can also be applied to OPs to improve quality. However, similarities and differences exist in how these charts are applied in different contexts (see Table 1):

Overall, while differences exist in how statistical control charts are applied in manufacturing processes and OPs, the underlying principles and goals of these charts are similar.

SPC can be used to control various parameters of an OP, including (1) *total process time (TPT)*, the time it takes to complete a process or activity; (2) *defect rate*, the proportion of service outcomes that are defective, fail to satisfy the customers or contain errors; (3) *throughput*, the rate at which a process can produce products or deliver services; (4) *customer satisfaction*, the level of customer satisfaction with a product or service; and (5) *total process cost (TPC)*, the cost of producing a product or delivering a service.

Table 1
Comparison of applications of SPC in manufacturing and operation processes.

Similarities	Differences
The basic principles of statistical control charts are the same regardless of whether they are applied to manufacturing processes or OPs. These principles include selecting the appropriate chart type, setting control limits, collecting and analyzing data, and taking corrective action when necessary.	The types of data collected in manufacturing processes and OPs may differ. Manufacturing processes may collect data on physical characteristics such as weight, dimensions, or color, while OPs may collect data on cycle time, customer satisfaction, or employee performance. Furthermore, one OP can contain multiple technological processes at the same time.
In both production and operation (for example, business) contexts, statistical control charts are used to detect and prevent defects or errors in the process.	The chart types used in each context may differ depending on the nature of the data being collected. The tasks of OPs often follow a nonnormal distribution because of the diverse nature of tasks from different subprocesses.
Both types of processes require ongoing monitoring and continuous improvement to maintain quality and prevent errors.	In manufacturing processes, the focus is on producing physical goods with the required quality, while in OPs, the focus is on providing services or delivering information with efficient utilization of resources to satisfy stakeholder needs. This may affect the types of errors that can occur and the methods used to prevent them.
	The sources of variability in each type of process may differ. In manufacturing processes, sources of variability may include variations in raw materials, machine settings, or operator performance, while in OPs, sources of variability may include variations in customer demand, employee skills, or software performance.

By using SPC to control these parameters, businesses achieve several advantages. *Improved quality*: SPC can help businesses identify and address process variations, which can lead to reduced defects and improved quality. *Increased efficiency*: By monitoring and controlling TPT and throughput, businesses can identify bottlenecks and other inefficiencies in their processes and take action to eliminate them. *Reduced costs*: SPC can help businesses identify and eliminate waste and other inefficiencies, leading to reduced costs and increased profitability. *Improved customer satisfaction*: By monitoring and controlling customer satisfaction levels, businesses can identify areas for improvement and take action to address them, leading to increased customer loyalty and retention. *Data-driven decision-making*: SPC provides businesses with objective data about their processes, allowing them to make data-driven decisions about how to improve their operations. When SPC is used to control the parameters of operation (business) processes, businesses can achieve significant improvements in quality, efficiency, cost, customer satisfaction, and decision-making.

To handle and control OPs, an OP modeling technique must be chosen. The most commonly used methods are business process model and notation (BPMN) (Dijkman et al., 2011), a graphical notation for representing OPs in a standardized way; event-driven process chain (EPC) diagrams (Amjad et al., 2018), a type of flowchart used to visualize OPs, particularly those that involve complex decision-making and multiple paths; data flow diagram (DFD) (Li and Chen, 2009), a visual representation of the data flow through a system or process; Value stream mapping (VSM) (Lasa et al., 2008), a lean manufacturing tool used to visualize and improve the flow of materials and information through a production process; and unified modeling language (UML) (Siau and Cao, 2001), a standardized modeling language used in software engineering to describe object-oriented systems and processes. We employed EPC, which can represent complex decision-making and multiple paths in a process. Unlike other process models, EPC diagrams can represent parallel processing paths and complex conditional logic in an easily understood manner. This ability makes EPC diagrams particularly useful for modeling processes that involve multiple departments or stakeholders and processes that are prone to bottlenecks and delays. Another advantage of EPC diagrams is their flexibility. They can be used to model high-levelOPs and detailed technical processes, making them versatile tools for process improvement and optimization. Overall, the event-driven process chain diagram is a powerful tool for visualizing and improving OPs, particularly those that are complex and involve multiple decision points.

This paper makes the following contributions to the literature.

C_1 We propose a new control chart for monitoring operation processes (OPs) that is applicable even when normality cannot be guaranteed.

C_2 We provide a fitting procedure for the proposed OP control chart and investigate its performance under nonnormality.

C_3 We analyze the performance of different distribution-free chart statistics to select the best basis for the OP chart.

C_4 We offer a recommendation scheme for the analyzed OP control charts to achieve better out-of-control performance.

C_5 We provide practical guidance for practitioners to control OPs and support decision-making for OP chart selection.

The remainder of the paper is organized as follows. Section 2 introduces the conceptual methods for OP modeling and the proposed control chart framework, including the simulation process for evaluation. Section 3 describes a practical application example from a machine repair process. Section 4 presents the results, first fitting the charts to real data and then using simulations to assess performance under various conditions. Finally, Section 5 summarizes the findings and conclusions.

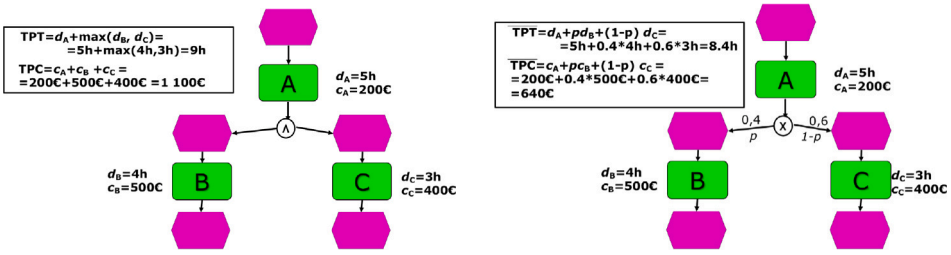
2. Methods

In this section, having established the need for a dedicated OP control chart, we describe the methods used to develop and evaluate its framework.

2.1. Business and operation process modeling

The EPC modeling technique is employed to describe business (operation) processes. In EPC, the main objects are as follows: (1) *Events* are occurrences that trigger a process or a subprocess. Events are represented as hexagons in the EPC diagram. (2) *Processes* represent the entire sequence of events and functions that make up an OP. Processes are represented as rounded rectangles in the EPC diagram. (3) *Logical operators* are used to define the conditions for events and functions. There are two types of logical operators: (a) the *AND operator* indicates that all conditions must be met before an event or function can be executed. (b) The *XOR (exclusive OR)* operator indicates that exactly one condition must be met before an event or function can be executed.

The AND operator allows parallel performance of tasks via parallel branches, whereas the XOR operator is called a decision operator because we have to decide which branch will be executed. OR operators indicate that at least one condition must be met before an event or function can be executed; this operator is rarely used and can be expressed as a combination of the XOR and AND operators.



(a) Simple EPC with AND (⋀) operators. (b) Simple EPC with XOR (X) operators.

Fig. 1. Simple EPC processes, where three tasks are scheduled with their duration (d) and cost (c).

In EPC, lead times and costs can be assigned only to processes. An event indicates only the trigger/starting or the result/completion of a process. With the XOR operator, probability or relative frequency values can be assigned to branches, where the total probability/relative frequency must be one when all branches are considered. Note that, depending on the conditional probability value, different processes are executed on different branches. Therefore, different processes must be controlled for in different outcomes of decisions. To demonstrate the proposed framework, we apply it to a simple OP modeled using EPC, as shown in Fig. 1, which connects conceptual design with practical use. Two examples of a simple OP modeled by EPC are shown in Fig. 1.

Two variants of the same OPs are shown in Fig. 1, where three tasks (A, B, and C) are connected via AND (Fig. 1(a)) and XOR (Fig. 1(b)) operators. (For example, these tasks could represent A: receipt and processing of customer complaints; B: isolation, locking and inspection of the affected item; and C: consultation with the customer to determine the fault more precisely and decide whether the complaint is legitimate.) The AND operator indicates that processes B and C will be executed in parallel after executing process A. The entire OP will be complete if each process is complete ($TPT = d_A + \max(d_B, d_C)$). Furthermore, costs arise regardless of whether serial or parallel operations are used ($TPC = c_A + c_B + c_C$). In contrast to the AND operator, in the case of the XOR operator, we can only calculate the expected values of TPT and TPC (denoted as $\overline{TPT}$ and $\overline{TPC}$, respectively) because branch B or branch C will be executed, with (conditional) probability values $p = 0.4, 1 - p = 0.6$. The calculation of the expected values of TPT ($\overline{TPT} = d_A + pd_B + (1-p)d_C$) and TPC ($\overline{TPC} = c_A + pd_B + (1-p)c_C$) assumes that these conditional probability values or relative frequencies resulted from the previous runs.

For real-world deployment, the OP chart can be integrated with enterprise or manufacturing information systems such as enterprise resource planning (ERP) and manufacturing execution system (MES) platforms, which are typically used to manage business and production processes. Data from these systems, such as process times or decision outcomes captured in EPC models, can be extracted via APIs and fed into the OP chart for real-time monitoring. This integration enables automated detection of out-of-control conditions and facilitates decision-making by linking chart signals to existing workflow tools. The EPC methodology is particularly well suited to this task, as it models processes for the purpose of developing information systems. The events that trigger or terminate activities in EPC can usually be extracted from the logs of ERP or MES systems. Starting with pilot-level implementations in sectors such as healthcare, finance, software development, and education to assess effectiveness is highly recommended, although challenges such as data compatibility and system latency require further exploration in practical settings.

2.2. Process control

In this paper, we investigate the performance of different control charts on OPs. The analyzed control charts are the (1) traditional Shewhart X-bar chart, (2) X-bar chart with permutation-computed control lines, (3) median chart and (4) standardized mean–rank (SMR) chart.

X-bar chart. The traditional Shewhart X-bar chart uses the sample means as the chart statistic. Let the number of samples be m; each sample has a size of n, and X_{ij} denotes the jth observation for the ith sample (where $i = 1, \ldots, m$ and $j = 1, \ldots, n$). The traditional X-bar chart assumes that X_{ij} follows a normal distribution with the expected value μ and standard deviation σ ($X_{ij} \sim N(\mu, \sigma)$). The upper and lower control limits (UCL and LCL, respectively) are calculated as follows (Goedhart et al., 2017):

$$UCL = \mu + k_\alpha \frac{\sigma}{\sqrt{n}} \tag{1}$$

$$LCL = \mu - k_\alpha \frac{\sigma}{\sqrt{n}} \tag{2}$$

where α is the false alarm probability (FAP), k is the control limit coefficient of the corresponding selected α value, and $k_\alpha = \phi^{-1}(1 - \alpha/2)$ and $\phi^{-1}(x)$ are the inverses of the standard normal cumulative distribution function.

Distribution-free X-bar chart. The distribution-free version of the X-bar chart (denoted the DF X-bar below) follows the same logic as the control chart does. The only difference is in the calculation of the control limits. While the traditional X-bar chart sets the control limits by selecting an α value and calculates k analytically afterward, the DF X-bar chart uses permutation to calculate the control lines. To obtain the control lines for the desired FAP, the permutations comprise the following steps: (1) Calculation of the selected control chart statistics from the observations, (2) permutation of the samples from the initial chart statistics without replacement and (3) determination of the control lines by averaging the $100(1-\alpha)$ percentile values (Ikpotokin and Ishiekwene, 2016). During the permutation, Monte Carlo simulation is performed; the goal is to find the optimal value for k to achieve a desirable value of FAP. The resulting control limits are distribution free (Capizzi and Masarotto, 2018).

Median chart. For the median chart, the sample median can be calculated as follows (Castagliola and Figueiredo, 2013):

$$\tilde{X}_i = \begin{cases} X_{i,(n+1)/2}, & \text{if } n \text{ is even} \\ \frac{X_{i,(n/2)} + X_{i,(n/2+1)}}{2}, & \text{if } n \text{ is odd} \end{cases} \tag{3}$$

where $\tilde{X}_i$ is the sample median for the ith sample. The control lines are calculated as follows:

$$UCL = \mu + k\sigma \tag{4}$$

$$LCL = \mu - k\sigma \tag{5}$$

Although initially, the control limits for the median chart are calculated with the formula defined above, in this paper, a permutation-based approach is used for the median chart calculated in the R program via the "dfphase1" package (Capizzi and Masarotto, 2018).

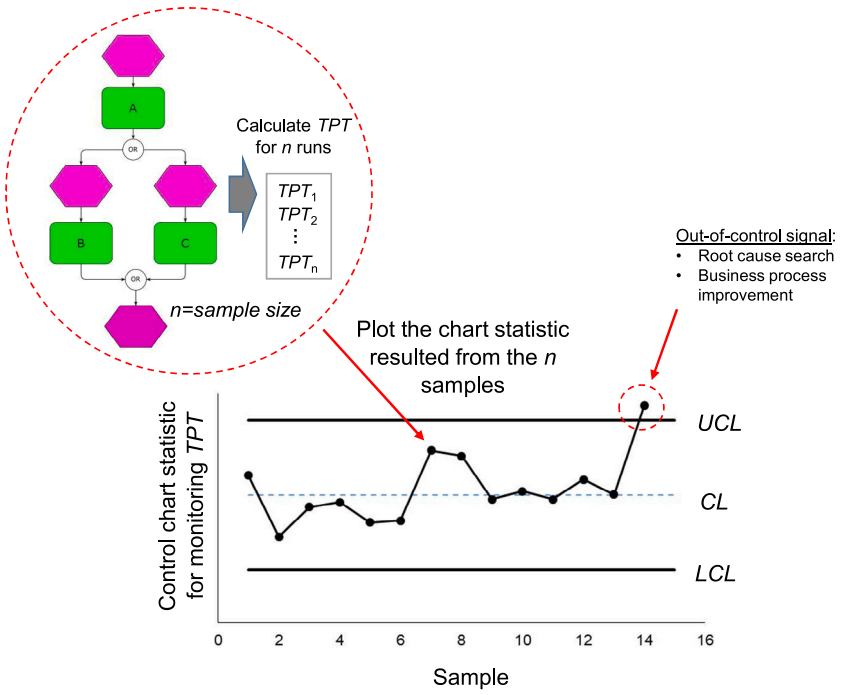


Fig. 2. Schematic figure of an operation process control chart.

Standardized mean rank chart. The standardized mean–rank chart (SMR chart in the following) assigns $R_{ij} = 1, 2, \ldots, N$ integer values to the X_{ij} observations on the basis of their ranks in the population, where the pooled sample size is N and $N = m \times n$ (in the case of ties, the midrank method is applied). The mean and variance of the rank values can be described as follows (Jones-Farmer et al., 2009):

$$\overline{R_{ij}} = \frac{N+1}{2} \tag{6}$$

$$var(R_{ij}) = \frac{(N-1)(N+1)}{12} \tag{7}$$

If they are calculated for samples, the mean and variance can be expressed as follows:

$$E(\overline{R_i}) = \frac{N+1}{2} \tag{8}$$

$$var(\overline{R_i}) = \frac{(N-n)(N+1)}{12n} \tag{9}$$

After standardization, the random variable

$$Z_i = \frac{\overline{R_i} - E(\overline{R_i})}{\sqrt{var(\overline{R_i})}} \tag{10}$$

follows a standard normal distribution on the basis of the central limit theorem if n is sufficiently large. For the SMR chart, the centerline is zero ($CL = 0$), and UCL and LCL are estimated via simulation, where the goal of the optimization is to achieve the desired FAP value.

2.3. Control charts for operation processes

In this study, we apply phase I charts and assume that the observed and control values are independent and identically distributed. Fig. 2 illustrates the logic behind the monitoring and control of an OP with a control chart.

The OPs, which are tracked and controlled, reoccur multiple times in a year, month or week. These OPs can have different subjects or clients or be performed with the same actors and items but have different decisions within the workflow modeled by the same EPC; thus, different routes of the EPC are activated. These routes can result in different throughput times, resource usages or operational costs. The aim of the OP chart is to monitor these repetitive processes, described with the same EPC, to distinguish what variances in the process measures are natural and what the products of systematic deviations and assignable causes are. The identification of assignable causes is the basis of process improvement through the elimination of causes of negative deviations or the exploitation of sources of positive deviations (e.g., by making good practices on the basis of these positive deviations). As Fig. 2 shows, each data point on the OP chart is obtained via observations and measurements of multiple instances of the same OP. In other words, an OP is specified and modeled with EPC, and characteristics such as TPT and TPC can be calculated after each complete run of the entire OP. The TPT or TPC values for each run can be structured into samples, and the control chart statistic can be calculated from the sample comprising n observations (see Fig. 2). If an out-of-control signal is detected, the chart indicates that the expected duration or the expected total cost of the OP has changed. In that case, a root-cause search must be performed to detect the assignable causes, and the process must be improved by eliminating the blocking factors. Note that TPT and TPC can be monitored; however, in Fig. 2, TPT is monitored as an illustration for simplicity. To monitor the OP, the OP chart type must be selected, and the control chart parameters must be designed. When analyzing OP data, it is important to consider that there may be cases where only one control limit is applicable. This statement is particularly true when the lower control limit falls below zero or when logically impossible conditions exist. The proposed chart fitting procedure is shown in Fig. 3.

As shown in Fig. 3, the proposed OP control chart design and application comprises six steps: (1) process modeling, (2) calculation of TPT and TPC, (3) normality testing, (4) control chart selection and design, (5) continuous data collection and (6) monitoring of the OP. In the following, we discuss these steps in detail.

(1) process modeling. First, the selected OP needs to be modeled through the determination of each process, subprocess, and event of the selected OP. In addition to the processes and events, all the logical operators, such as AND, OR, and XOR, must be specified to ensure that all possible parallel runs and decisions are identified in OP. In this step, the EPC diagram can be used for OP modeling.

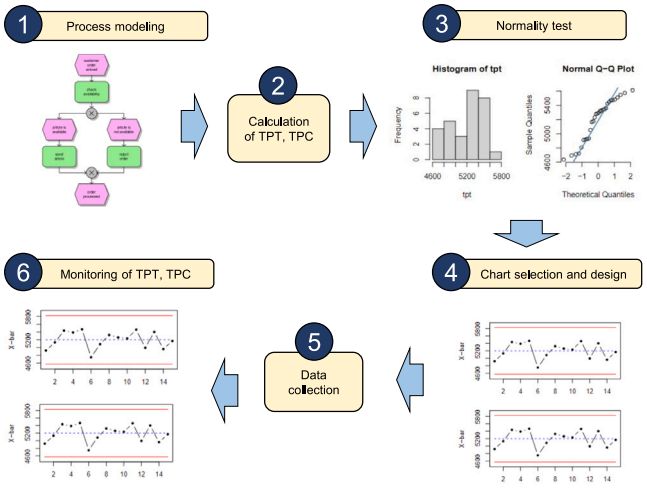


Fig. 3. Control chart fitting procedure.

(2) calculation of TPT ***and*** TPC. Using the structure of OP specified in step (1), the TPT and TPC of the process are calculated as described in Section 2.1. At this step, the data must be observed multiple times, and TPT and TPC must be calculated for each run. These necessities emerge because, in the following steps, the first TPT and TPC series constitute the basis for calculations such as normality tests and control chart phase 1 analysis. At this step, we recommend performing at least 30 observations for running the selected OP. This action generates at least 30 TPT and TPC values, which is the minimum required number of data points for several normality tests.

(3) normality test. An OP comprises several tasks (processes), each of which can follow a certain type of distribution in terms of cost or duration; thus, it cannot be guaranteed that the aggregated OP's TPT and TPC are normally distributed. Normality testing is important since it determines whether a traditional Shewhart chart can be used, such as an X-bar chart, or whether selecting and designing a distribution-free control chart is necessary. To conduct the normality test, we suggest using the Shapiro–Wilk test because it has good power properties and is a widely used method for testing normality (Das and Imon, 2016). The Shapiro–Wilk test is based on the correlation between the observed data values and the corresponding normal scores. The test statistic can be formulated as follows:

$$W = \frac{(\sum a_i y_i)^2}{\sum (y - \overline{y})^2} \tag{11}$$

where y_i is the ith observed order statistic and a_i is the corresponding expected normalized order statistic. In the case of normality, the value of W is close to 1; during hypothesis testing, normality is rejected if W is significantly less than 1. The Shapiro–Wilk test was developed for testing normality; however, it is important to test whether a sample follows a specified theoretical distribution outside the normal distribution. For this purpose, the Kolmogorov–Smirnov test is widely used. The test statistic, denoted as D, can be defined as follows (Das and Imon, 2016):

$$D = sup_x |F_n(X) - F(X)^*| \tag{12}$$

where $F_n(X)$ denotes the empirical distribution function of the sample and $F(X)^*$ is the assumed theoretical distribution function. A large value of D indicates that the sample follows a different distribution than the theoretical distribution. The Kolmogorov–Smirnov test applies to continuous cases. In the case of a discrete task duration distribution, the chi-square test can be used to test the distribution type. The test statistic is calculated as follows:

$$\chi^2 = \sum_{i=1}^{r} \frac{(n_i - n_i^*)^2}{n_i^*} \tag{13}$$

where r is the number of categories and n_i^* is the expected number of elements (based on a theoretical distribution) in category i, where n_i is the observed number of elements.

In addition to statistical tests, normality can be tested visually. The Q–Q (quantile–quantile) plot is an excellent tool for visually examining the differences between theoretical and observed distributions. The Q–Q plot is a straight line representing the best fitting case, which is when the theoretical and observed quantiles are equal.

(4) control chart selection and design. In this step, the proper control chart is selected to control OP. If step (3) confirms a normal distribution, the Shewhart X-bar chart can be used since the assumptions are fulfilled, and this chart is also a good choice because of its simplicity. Otherwise, a distribution-free control chart needs to be selected. To select the best-performing distribution-free control chart, the in-control average run length (ARL_0) and out-of-control average run length (ARL_1) values can be considered. Control chart performance is affected by various factors, such as the size of the expected process shift or sample size. The ARL values can be estimated through simulations. In this paper, we provide recommendations for selecting the best-performing control chart to control the OP sample size and expected shift size. To obtain the rules for selecting the best performing control chart considering different process parameters, such as sample size or process shift size, the decision tree algorithm is used. Decision trees are used in computer science to reveal the influencing features and extract patterns in large datasets. Decision trees recursively partition the feature space to find a set of decision rules that provide an informative and robust hierarchical classification scheme (Myles et al., 2004).

(5) continuous data collection. After the control chart is selected and designed, i.e., the sample size is chosen, the control limits are calculated, and phase 1 analysis ends. To monitor and, if necessary, control the OP, continuous data collection related to the TPT and TPC values is needed. In this step, the integration of an enterprise resource planning (ERP) system can automate the calculation of the entire OP duration and cost every time OP ends. The calculation of the TPT or TPC values is not computationally intensive, and for most OPs, requires several orders of magnitude less time than the lead time or frequency of occurrence of OP. Data collection could be a challenge, especially for workflows and activities that are not logged directly in an ERP or other information system. These data are subject to measurement uncertainty, perturbation, noise, or delay in registration.

(6) monitoring of TPT ***and*** TPC. If the data are collected continuously, each new TPT and/or TPC value can be plotted on its corresponding OP chart. In an out-of-control situation, the assignable cause of the shift must be investigated, and correctional intervention should be performed.

2.4. Simulation process

To evaluate the performance of each control chart, simulations are conducted to obtain the ARL_0 and ARL_1 values. The steps of the simulations are described below.

ARL_0 evaluation:

1. Perform distribution identification for each task in OP.
2. Generate the TPT series via Monte Carlo simulation.
3. Fit the control chart to the simulated TPT.
4. For each control chart, determine the location of the first point indicating a (false) out-of-control signal (run length).
5. Iterate steps 2–4 and save the run length values for each control chart from each iteration.
6. Calculate the average (median and standard deviation) of the run length values to obtain ARL_0 (MRL_0 and $SDRL_0$) for each control chart.

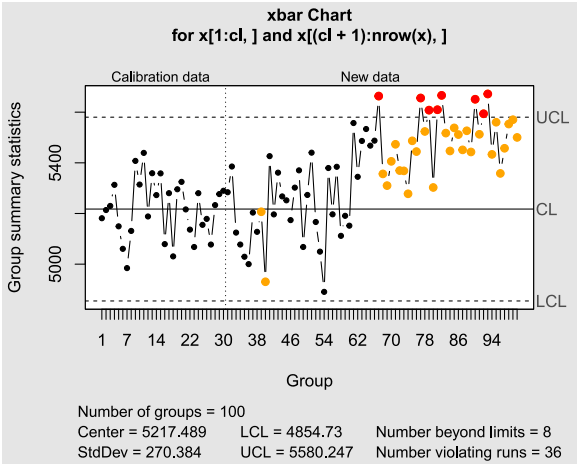


Fig. 4. Example of a simulated process shift.

For a given OP (real-life example), the *PearsonDS* R package is used to estimate the four moments of the distribution: the mean, standard deviation, skewness and kurtosis. After the four moments of the distribution for each task are obtained, random duration values are generated with the estimated distribution (using the four estimated moments). The simulated TPT is calculated in each iteration as the aggregation of the generated durations, as discussed in Section 2.1. Each analyzed control chart is fitted to the simulated TPT series with a given sample size. The ARL_0 value is calculated for each control chart as described in steps 4–5. This simulation is conducted for different sample sizes for each control chart.

ARL_1 evaluation:

1. Perform distribution identification for each task in OP.
2. Generate the TPT series via Monte Carlo simulation.
3. Simulate a shift in the series with a selected shift size, starting at a given location.
4. Calculate the limits for each control chart considering the first m chart statistics before the shift occurs.
5. Calculate the length from the shift starting point to the first out-of-control signal (run length).
6. Iterate steps 2–5 and save the run length values for each control chart from each iteration.
7. Calculate the average (median and standard deviation) of the run length values to obtain ARL_1 (MRL_1 and $SDRL_1$) for each control chart.

The structure of the simulation is similar to that of the simulation related to ARL_0 estimation. The most important difference is shift generation. The shifted TPT series is described as follows:

$$TPT_s(i) = \begin{cases} TPT_g(i), & \text{for i} < l \\ TPT_g(i) + z\sigma, & \text{for i} \geq l \end{cases} \tag{14}$$

where $TPT_g(i)$ is the ith value of the generated TPT series, $TPT_s(i)$ is the ith value of the shifted TPT series, σ is the standard deviation of the controlled process, l is an integer representing the location of the shift as the lth value of TPT_g, and z is a coefficient representing the shift size in terms of standard deviation. An example of a generated process shift is shown in Fig. 4.

An X-bar chart is shown in Fig. 4, where the first 30 samples are used to calibrate the chart, i.e., calculate the centerline and the control limits. A $z = 1.5$ shift occurs after the 60th sample, and the chart detects the shift at the 67th sample; therefore, the run length is 7 in this case. This iteration is repeated several times, and the ARL_1 value is estimated as the average of the run length values given by each iteration. The simulation is conducted with different sample sizes (n) and different shift sizes (z). Having outlined the conceptual framework and methods for designing and simulating OP control charts, we now apply these ideas to a real-world example. This application demonstrates how the proposed charts perform in an operational setting involving a machine repair process, highlighting their practical utility before evaluating broader performance through simulations.

3. Description of a practical example

In this section, we present a practical example of a machine repair process comprising 36 tasks. The goal of this section is to provide an overview of a practical example, which we use in Section 4, to demonstrate control chart usage in an operational environment and to investigate control chart performance. We selected this process as an example because it involves diverse types of operational tasks, including reparation, planning, and invoice creation. In this way, we can use and analyze various control charts in an adequately complex environment. For more details about the operational process, we also provide a table including the definitions for each step included in the process in the supplementary material B.11. An additional practical example is also provided in Appendix C.

The structure of OP is shown in Fig. 5.

The machine repair process for production equipment comprises 9 larger blocks. In the first block, the damage is assessed, including the failed components, parts and failure modes; then, the process is divided depending on whether the given machine has a warranty. In the case of a warranty, repair begins (Block 7); this repair can be performed on site (Block 6) or at the site of the operator's maintenance partner (Block 5). If the given machine has no warranty, a price offer will be made (Blocks 2, 3, and 4), after which the repair can be performed at the site of the company or the operator's maintenance service partner. After a successful repair, documentation is performed (Block 8), and then the equipment is restarted (Block 9).

Each task duration is independent of the previous task duration, and each duration has its own distribution, where normality cannot be guaranteed. Table 2 provides descriptive statistics for each task of the process, where the values represent the duration in minutes.

As Table 2 shows, tasks t_9, t_{24}, and t_{25} have significantly higher mean values than the overall average. This finding indicates that these tasks should be considered carefully because their delay can significantly affect the overall TPT. To observe the differences in the task variances, Fig. 6 is presented, where the x-axis represents the task number and the y-axis represents the standardized values for each task. The color of each box is set on the basis of the group median.

As Fig. 6 shows, there are several strongly skewed distributions, such as those for tasks t_{23} and t30. Extreme values can be observed only for tasks t_3, t_6 and t_{34}. The data in Fig. 6 also suggest that several tasks are skewed; thus, normality cannot be fulfilled in these cases, and therefore, the overall TPT values are highly unlikely to follow a normal distribution. TPT is calculated as the aggregation of the task durations, as described in Section 2:

$$\begin{aligned} TPT = & \sum_{1}^{6} t_i + 0.7^* \sum_{7}^{12} t_i + 0.7^*0.2 \sum_{13}^{14} t_i + 0.7^* \sum_{15}^{16} t_i + 0.7^*0.7 \sum_{17}^{20} t_i \\ & + 0.7^*0.7^*0.1^* \sum_{21}^{22} t_i + 0.7^*0.7^* t_{23} + 0.3^* \sum_{24}^{25} t_i + 0.3 \\ & + 0.7^*0.7^* \sum_{26}^{28} t_i + 0.7^*0.3^* t_{29} \\ & + 1^*0.1^* \sum_{30}^{31} t_i + 1^*0.9^* \sum_{32}^{36} t_i \end{aligned} \tag{15}$$

where the multiplicators are derived from the probabilities of execution related to the specific operator. The execution probabilities were estimated by experts at the company, considering historical data. From a historical dataset, 30 runs of the machine repair process were collected,

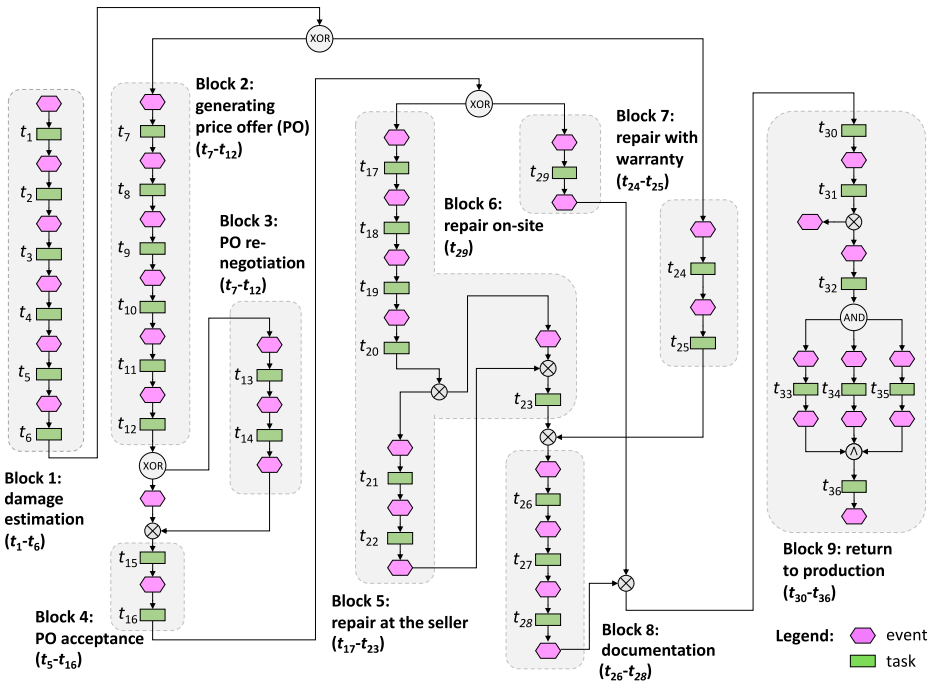


Fig. 5. Process flow diagram of the machine repair process. The gray blocks represent the main task groups.

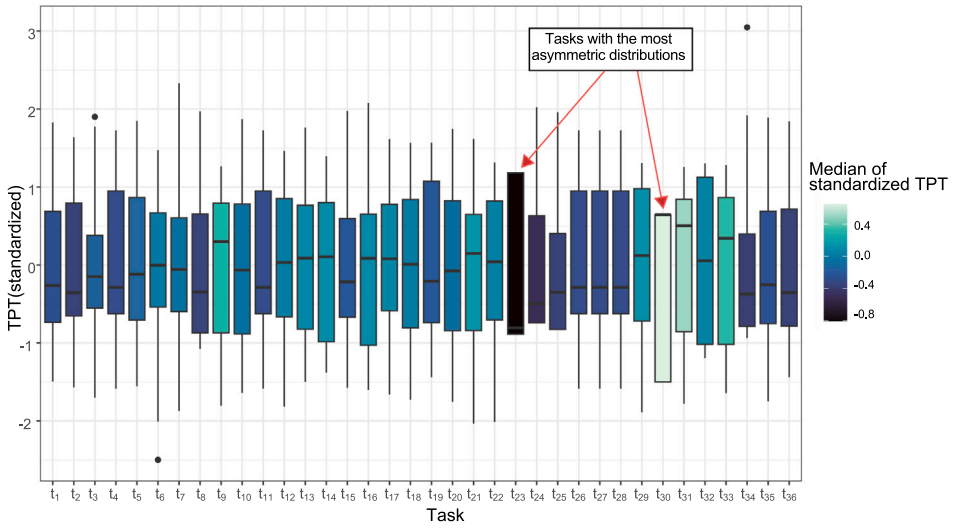


Fig. 6. Dispersion of standardized TPT values per task. The color of the boxes represents the median of the standardized task durations, the vertical lines represent the range of durations per task, and the black dots denote outliers. (For interpretation of the references to color in this figure legend, the reader is referred to the web version of this article.)

and TPT was calculated for each run via Eq. (15). The average TPT related to the collected data was 5199 [min].

At the company, the data collection and registration of the duration values are supported by the company's integrated information system. After 30 data points (TPT values) were collected, the taskwise durations were exported to an Excel spreadsheet for each run. After data collection and analysis, the proposed OP chart was fitted to the machine repair process. Control chart usage in an operation process such as machine repair is highly valuable since without this information, the monitoring and control of the process and the identification of weak or risky tasks are difficult or even impossible. With the machine repair process as our practical example, we now turn to the results. In the following section, we first fit the proposed control chart methodology to the real dataset to assess its applicability. To gain a deeper understanding of long-term performance under varying conditions, we conduct simulations on the basis of the methods described in Section 2.4.

4. Results and discussion

4.1. Control chart fitting to real data

First, it is important to analyze the distribution type of the TPT as the control characteristic. The distribution of the TPT is shown in Fig. 7.

As shown in Fig. 7A, the histogram is skewed, which suggests that normality cannot be guaranteed during process control. The data in Fig. 7B confirm this observation because the dots fit poorly with the Q–Q line. To statistically confirm these observations, the Shapiro–Wilk normality test is conducted via Eq. (11). The test statistic results in

Table 2
Descriptive statistics for each task in the dataset.

Task	Min.	Max.	Mean	St. Dev.
t_1	0.50	3.60	1.90	0.93
t_2	8.00	15.00	11.43	2.18
t_3	90.00	119.00	103.70	8.05
t_4	30.00	35.10	32.44	1.54
t_5	30.00	34.50	32.06	1.32
t_6	54.98	72.60	66.06	4.43
t_7	27.30	37.60	31.89	2.45
t_8	20.50	25.30	22.20	1.58
t_9	1635.00	2860.00	2355.13	398.61
t_{10}	61.00	119.00	88.10	16.50
t_{11}	30.00	35.10	32.44	1.54
t_{12}	30.00	34.70	32.60	1.43
t_{13}	61.50	113.70	85.51	16.00
t_{14}	4.90	6.30	5.60	0.50
t_{15}	30.10	34.80	32.19	1.32
t_{16}	68.30	196.00	123.83	34.70
t_{17}	60.50	116.10	88.69	16.96
t_{18}	91.40	119.10	105.93	8.40
t_{19}	30.20	34.60	32.31	1.46
t_{20}	30.30	45.00	37.67	4.20
t_{21}	60.10	72.90	67.23	3.51
t_{22}	30.20	34.90	33.04	1.41
t_{23}	108.30	119.70	113.19	5.50
t_{24}	4003.00	4121.00	4034.63	42.66
t_{25}	4003.00	4126.00	4039.47	44.16
t_{26}	30.00	35.10	32.44	1.54
t_{27}	30.00	35.10	32.44	1.54
t_{28}	30.00	35.10	32.44	1.54
t_{29}	166.50	180.50	174.77	4.38
t_{30}	203.60	238.50	228.04	16.24
t_{31}	59.90	75.60	69.10	5.17
t_{32}	4.90	6.30	5.57	0.56
t_{33}	4.90	6.30	5.69	0.48
t_{34}	20.50	25.80	21.75	1.33
t_{35}	8.00	15.30	11.51	2.01
t_{36}	0.50	3.60	1.86	0.94

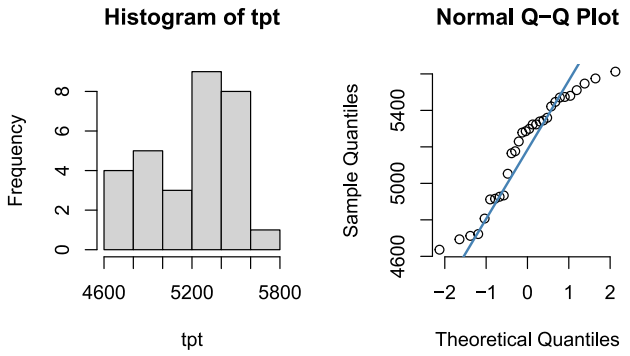


Fig. 7. Distribution of the TPT.

$W = 0.92$ with a significance level of $p = 0.022$; therefore, the test also confirms that the null hypothesis (the existence of a normal distribution) can be rejected and that TPT does not follow a normal distribution. This result is important from the control chart selection perspective since it indicates that traditional Shewhart charts may not perform well because of their limitations regarding normality. Instead of focusing on these control charts, distribution-free solutions must be considered during chart selection. In this example, we compare the performance of multiple distribution-free control charts with that of the traditional Shewhart X-bar chart. In this work, three distribution-free control charts are tested in addition to the traditional X-bar chart: (1) the distribution-free X-bar chart (denoted as the *DF X-bar chart* below), where the control limits are calculated through permutation; (2) the median chart; and (3) the SMR control chart. Fig. 8 shows the control charts fitted to OP.

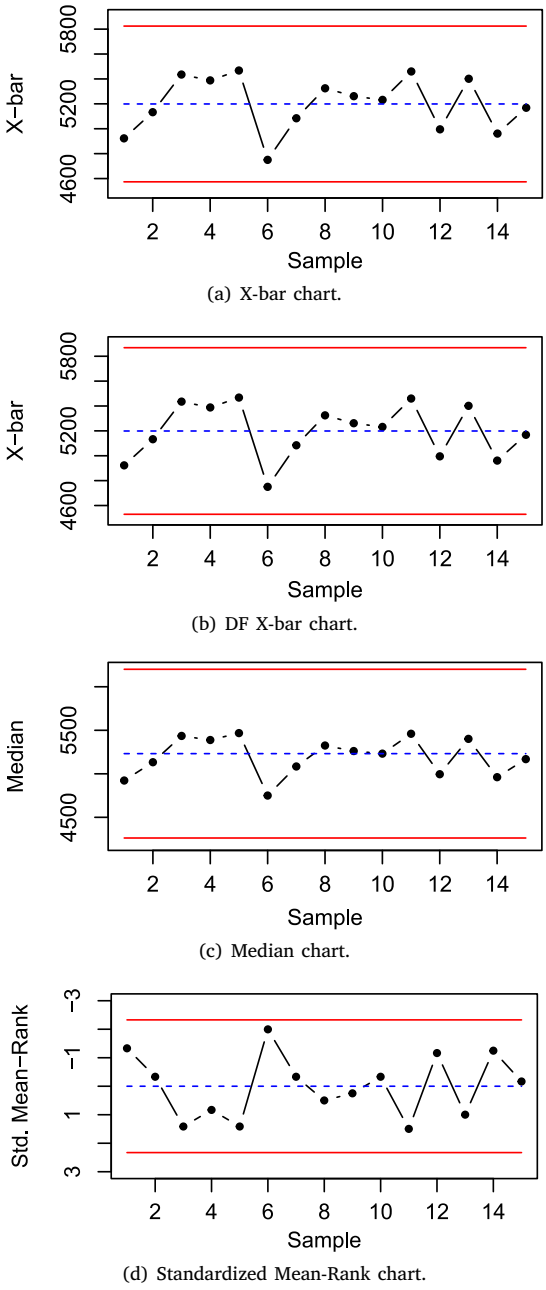


Fig. 8. Fitting control charts to monitor the TPT. The black dots represent the sample statistics, the red lines denote the UCL and LCL, and the blue dashed line is the centerline of the chart. (For interpretation of the references to color in this figure legend, the reader is referred to the web version of this article.)

As Fig. 8 shows, the control chart patterns are very similar for the X-bar, DF X-bar and median charts (Fig. 8A–C) and the SMR chart differs only in terms of the control chart pattern (Fig. 8). None of the four control charts indicate an out-of-control signal; however, differences exist in the width of the acceptance interval. The DF X-bar charts show only a slight difference related to the control limit values, whereas the median chart operates with a more relaxed control strategy. The SMR chart has the strictest control interval of the control charts considered. This observation suggests that the median chart could be a good choice when the goal is to achieve the maximum ARL_0 value (strong in-control performance) and the SMR chart is the best choice for minimizing ARL_1, i.e., achieving the fastest reaction in detecting a

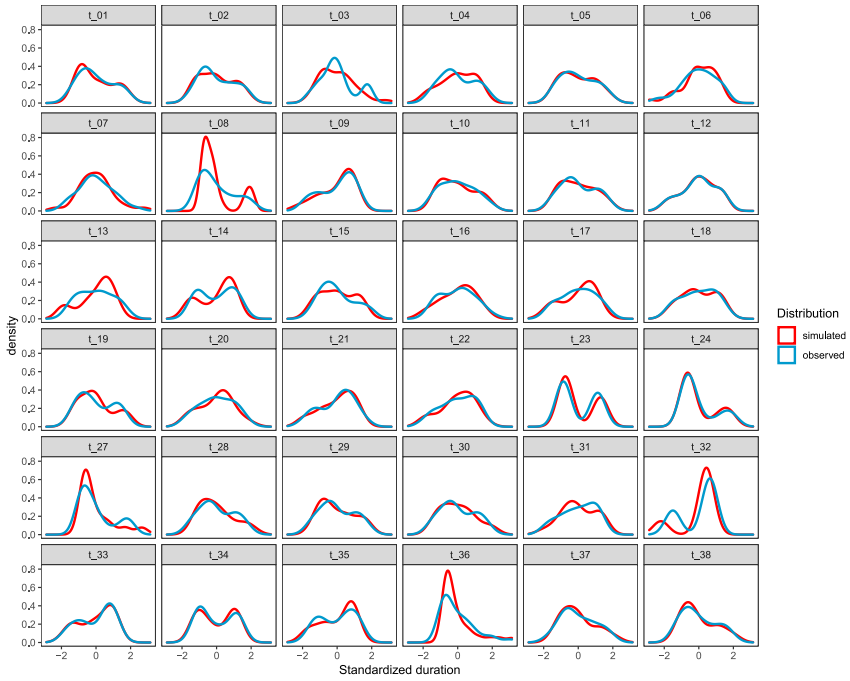


Fig. 9. Density plot of real vs. simulated durations.

Table 3
Calculated limits of the fitted control charts.

Chart	CL	LCL	UCL
X-bar	5217.49	4854.73	5580.247
DF X-bar	5199.01	4529.49	5868.54
Median	5231.69	4262.385	6201.00
SMR	0.00	−2.33	2.33

process shift. Table 3 shows the exact values of the center, lower, and upper control lines of the four fitted control charts.

As Table 3 also confirms, the mean rank chart has the narrowest control interval (good for achieving a small ARL_1), whereas the median chart has the widest interval (beneficial for a high ARL_0). Nevertheless, analyzing long-term average run lengths using simulations is necessary to draw more reliable conclusions.

4.2. Simulation results

To analyze the performance of the proposed control charts on the OP, a simulation is used. As the first step of the analysis, the distributions of the 38 tasks must be identified. Therefore, the four moments of each distribution are estimated. The *PearsonDS* R package was applied for the estimation. To test the goodness of fit of the simulated and real data series, the distributions are compared. The densities of the duration values related to the real and simulated data series are shown in Fig. 9.

As shown in Fig. 9, the distribution moments are adequately estimated, and the resulting simulated series are close enough to the real situation to model the selected OP. As shown in Fig. 9, the distributions of the durations related to certain tasks clearly follow various distribution types, such as centered distributions, strongly skewed distributions and distributions with multiple peaks, resulting in the aggregated TPT values following a mixed distribution. To investigate whether the simulated distributions are comparable to the real distributions, statistical tests were used, and the results are summarized in Table 4.

During the goodness-of-fit tests, three tasks are found (t_{23}, t_{24}, and t_{32}), for which the data show discrete patterns, and the Kolmogorov–Smirnov test cannot be performed because of the ties in the data values. For these cases, we run chi-square tests to examine whether the simulated and real distributions are the same. As Table 4 shows, the p values are greater than 0.05 for all the tasks; therefore, the statistical tests also confirm that the simulated series are good estimates of the real data. After the goodness of fit is checked, the control charts are designed, and the ARL_0 values are estimated. Table 5 shows the parameters of the simulation.

Table 6 shows the control chart parameters calculated during the simulation for each control chart. The control limits are mean values indicating the average value calculated from one thousand iterations.

After the durations and the TPT series are simulated, ARL_0 is estimated for each chart with different sample sizes. The simulation results are shown in Fig. 10. Fig. 10A shows the expected ARL_0 value for each control chart considering different sample sizes, and Fig. 10B illustrates the dispersion of the ARL_0 values with box plots.

Table 4
Results of the nonparametric statistical tests.

Kolmogorov–Smirnov test					
Tasks 1–19			Tasks 1–38		
Task	D	p-value	Task	D	p-value
t_1	0.100	0.999	t_{20}	0.133	0.952
t_2	0.167	0.799	t_{21}	0.133	0.952
t_3	0.200	0.586	t_{22}	0.133	0.952
t_4	0.167	0.799	t_{27}	0.333	0.071
t_5	0.100	0.998	t_{28}	0.100	0.998
t_6	0.133	0.958	t_{29}	0.100	0.998
t_7	0.100	0.998	t_{30}	0.200	0.586
t_8	0.100	0.998	t_{31}	0.133	0.952
t_9	0.133	0.958	t_{33}	0.133	0.952
t_{10}	0.133	0.952	t_{34}	0.300	0.134
t_{11}	0.200	0.586	t_{35}	0.167	0.799
t_{12}	0.167	0.799	t_{36}	0.167	0.799
t_{13}	0.133	0.958	t_{37}	0.133	0.952
t_{14}	0.133	0.952	t_{38}	0.133	0.952
t_{15}	0.167	0.799	Chi-square test		
t_{16}	0.167	0.808	Task	χ^2	p-value
t_{17}	0.067	1.000	t_{23}	107.859	0.980
t_{18}	0.133	0.952	t_{24}	510.000	0.417
t_{19}	0.167	0.799	t_{32}	1.236	0.744

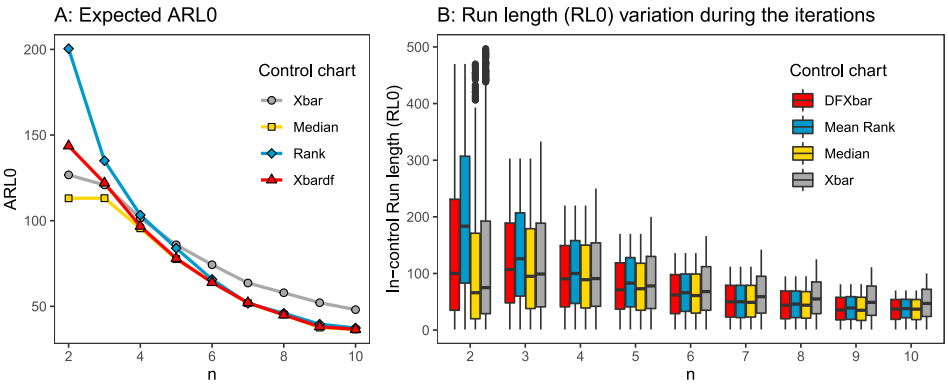


Fig. 10. In-control ARL based on the simulation.

Table 5
Simulation parameters for ARL_0 performance.

Parameter	Value
Iteration by control chart	1000
Sample sizes (n)	[2, 3, 4, 5, 6, 7, 8, 9, 10]
Samples to estimate control limits	30
Length of simulated TPT series	1000
Nominal ARL_0	~370
False alarm rate (α)	0.0027

Table 6
Control chart parameters during the simulation.

n	X-bar			SMR		
	$\overline{CL}$	$\overline{LCL}$	$\overline{UCL}$	$\overline{CL}$	$\overline{LCL}$	$\overline{UCL}$
2	5199.84	4623.11	5776.58	0.00	−2.35	2.35
3	5195.65	4714.39	5676.92	0.00	−2.66	2.66
4	5197.61	4788.55	5606.66	0.00	−2.81	2.81
5	5199.21	4835.22	5563.20	0.00	−2.89	2.89
6	5196.03	4872.69	5519.36	0.00	−2.94	2.94
7	5200.57	4906.75	5494.39	0.00	−2.97	2.97
8	5193.70	4921.44	5465.96	0.00	−2.99	2.99
9	5199.00	4946.40	5451.60	0.00	−3.01	3.01
10	5200.57	4965.60	5435.53	0.00	−3.02	3.02
n	DF X-bar			Median		
	$\overline{CL}$	$\overline{LCL}$	$\overline{UCL}$	$\overline{CL}$	$\overline{LCL}$	$\overline{UCL}$
2	5199.84	4600.67	5799.01	5211.25	4469.63	5952.88
3	5195.65	4695.06	5696.25	5204.78	4655.39	5754.18
4	5197.61	4766.43	5628.79	5206.35	4748.92	5663.79
5	5199.21	4812.06	5586.36	5205.28	4802.83	5607.72
6	5196.03	4849.76	5542.30	5200.91	4840.36	5561.47
7	5200.57	4879.63	5521.51	5203.47	4866.69	5540.24
8	5193.70	4892.17	5495.23	5197.53	4885.11	5509.95
9	5199.00	4915.72	5482.28	5200.49	4905.97	5495.01
10	5200.57	4932.81	5468.32	5204.14	4926.52	5481.75

As shown in Fig. 10A, the distribution-free control charts outperform the conventional X-bar chart when the sample size is smaller than 5. The best solution is the SMR chart for a small sample size when $n = 2$, which achieves an ARL_0 value that is almost twice as large as that of the X-bar chart. Fig. 10B also shows that after $n = 5$, the boxes for the distribution-free control charts overlap the interval related to the traditional X-bar chart. This finding can be explained by the effect of the central limit theorem. Specifically, the distributions of the samples with larger sample sizes ($n > 5$ in this case) tend toward a normal distribution, which equalizes the performances of the parametric and nonparametric control charts. To confirm this observation, the distributions of the control chart statistics for different sample sizes were analyzed with the Shapiro–Wilk normality test. Table 7 shows the results of this analysis.

As Table 7 shows, the normality test indicates that the samples follow a normal distribution if $n \geq 5$, which confirms the effect of the central limit theorem in this case. The ARL_0 and the in-control median and standard deviation run length values (MRL_0 and $SDRL_0$) are estimated, as shown in Table 8. The MRL_0 and $SDRL_0$ values are calculated for different sample sizes. The last two columns show the best performance on the basis of the maximum MRL_0.

Table 7
Results of the normality tests for different sample sizes.

n	W	p	$p > 0.05$
2	0.974	0.000	
3	0.986	0.005	
4	0.982	0.007	
5	0.986	0.080	*
6	0.981	0.059	*
7	0.988	0.452	*
8	0.989	0.585	*
9	0.978	0.182	*
10	0.980	0.331	*

As Table 8 shows, the findings are confirmed by the MRL_0 values, indicating that the SMR chart has the best performance with low sample sizes, but the X-bar chart can also be used as n increases. In contrast, the median chart is a considerable choice when stability is important in the decision ($SDRL_0$).

To measure the performance in detecting out-of-control signals, the out-of-control ARL values (denoted ARL_1) were computed during an additional simulation. In this simulation, 30 samples were used to calibrate the control chart (by determining the centerline and control limits), and each control chart was generated 1000 times to estimate the ARL_1 values for different shift sizes and sample sizes. The simulation parameters are listed in Table 9.

For the shift size selection, we covered all the small, medium and large shift size intervals. To this end, we followed the strategy used by Muñoz et al. (2023) to specify the interval from zero to 3. We use smaller steps for the lower section of the interval to obtain better interpretable results when the shift is more difficult to detect.

The 11 values for different shift sizes are presented in Figure ARL_1. The colors of the lines represent the control chart type, and each section of this figure shows the calculation for a specific sample size.

As Fig. 11 shows, the SMR chart has the best performance, with the lowest ARL_1 value in the case of $n \leq 7$. If $n > 7$, the performance measures of the control charts approach one another regardless of the size of the shift. The shift size also has a significant influence. If the shift size is greater than one, distribution-free control charts do not have an advantage over the traditional X-bar chart. On the basis of the results, the following recommendations can be provided: To control an OP for which normality cannot be guaranteed, if the sample size is small, i.e., $n < 5$, a nonparametric control chart should be used, such as the SMR, median or distribution-free X-bar chart. For moderate sample sizes such as $5 \leq n < 8$, only the SMR chart is recommended since only

Table 8
Control chart in-control performances.

n	Median		Mean- Rank		X-bar		DF X-bar		Best
	MRL_0	$SDRL_0$	MRL_0	$SDRL_0$	MRL_0	$SDRL_0$	MRL_0	$SDRL_0$	MRL_0
2	117.00	129.09	139.00	113.77	68.00	105.84	87.00	99.15	SMR
3	119.00	77.49	139.50	80.62	82.50	83.95	117.00	78.73	SMR
4	78.00	69.20	80.00	71.72	64.00	60.99	80.00	63.42	SMR
5	87.50	56.84	80.00	43.50	86.50	55.40	80.00	47.38	Median
6	46.00	47.04	36.00	43.33	66.50	45.02	44.00	45.31	Xbar
7	69.00	36.21	45.00	33.92	61.00	39.46	56.00	34.71	Median
8	30.00	21.56	53.00	27.71	50.00	33.43	29.50	21.87	SMR
9	58.00	23.86	51.00	18.30	58.00	30.64	49.00	23.18	Median
10	18.00	16.73	18.00	21.50	43.50	28.64	24.00	19.47	Xbar

Note: nominal ARL_0 is set to ~370 ($\alpha = 0.0027$ resulting $k = 3$).

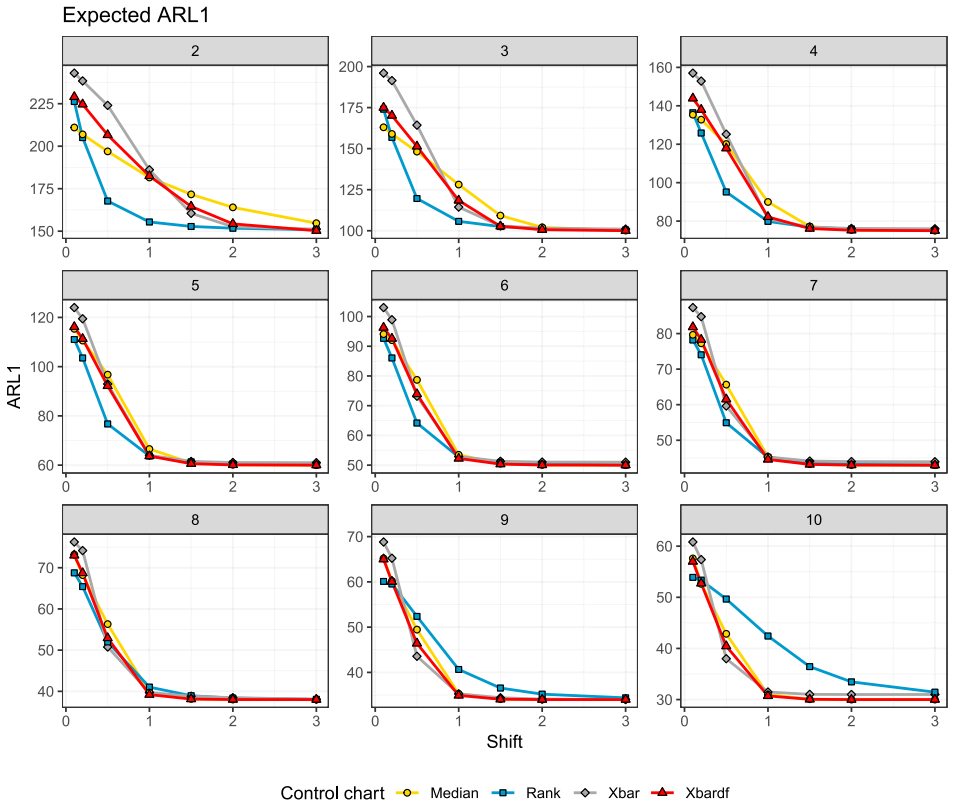


Fig. 11. Out-of-control ARL based on the simulation. (For interpretation of the references to color in this figure legend, the reader is referred to the web version of this article.)

Table 9
Simulation parameters for ARL_1 performance.

Parameter	Value
Iteration by control chart	1000
Sample sizes (n)	[2, 3, 4, 5, 6, 7, 8, 9, 10]
Shift sizes (z)	[0.1, 0.2, 0.5, 1, 1.5, 2, 3]
Shift location (ith sample)	300
Samples to estimate control limits	30
Length of simulated TPT series	1000
Nominal ARL_0	~370
False alarm rate (α)	0.0027

this nonparametric chart has significantly better performance than the traditional X-bar chart does. Finally, for large sample sizes ($n > 7$), a nonparametric control chart does not result in better performance than the traditional X-bar chart does, regardless of the shift size. Like ARL_0, the out-of-control run weights are also analyzed with MRL_1 and $SDRL_1$, as shown in Table 10.

Table 10 also confirms the observation from Fig. 11. The X-bar and DF X-bar charts have the best performance with greater z; however, increasing the sample size generally reduces the performance differences among the analyzed control charts if MRL_1 and $SDRL_1$ are considered measures of performance.

For a clearer presentation of the recommendations, we conducted a decision tree analysis, where the dependent variable is the control chart with the minimal ARL_1 and the independent variables are the sample size (n) and shift size (z). The resulting decision tree structure is shown in Fig. 12.

The characteristics of the decision tree are also worth analyzing. The error of trees of different sizes is shown in Fig. 13. The upper x-axis shows the size of the tree (number of terminated nodes), and the lower x-axis denotes the cp score, which is a complexity measure of the tree.

The algorithm uses complexity measures as stoppage criteria for tree growth. To prevent overfitting, in this case, the cp value for the current tree size is above the default stoppage value; therefore, the tree size can be accepted at a size of four since it is near the geometric mean of the cp values calculated from cross-validations, and keeping it at the greatest available depth provides more detailed insight for understanding the selection rules.

Table 10
Control chart out-of-control performances.

n	z	DF X-bar		SMR		Median		X-bar		Best MRL_1[a]
		MRL_1	$SDRL_1$	MRL_1	$SDRL_1$	MRL_1	$SDRL_1$	MRL_1	$SDRL_1$	
2	0.1	306.50	129.29	204.00	81.61	**193.00**	52.76	198.00	91.44	M
	0.5	190.00	84.64	**159.00**	27.95	163.50	52.92	174.00	92.42	SMR
	1	159.00	53.90	**153.00**	7.25	154.00	29.07	159.00	60.18	SMR
	1.5	153.00	27.69	**152.00**	3.15	153.00	32.83	153.00	21.06	SMR
	2	**151.00**	24.65	**151.00**	1.93	152.00	38.16	152.00	4.09	DFX, SMR
	3	**150.00**	0.94	**150.00**	1.16	150.00	9.59	151.00	0.47	DFX, SMR
3	0.1	177.50	68.58	**162.00**	60.68	177.50	71.06	173.00	67.26	SMR
	0.5	135.00	53.94	**111.00**	23.23	147.00	64.53	144.00	59.52	SMR
	1	107.00	29.06	**103.00**	7.17	111.00	40.90	107.00	17.21	SMR
	1.5	**101.00**	5.80	102.00	3.18	102.00	20.03	102.00	2.75	DFX
	2	**100.00**	1.19	101.00	1.84	101.00	10.06	101.00	0.91	DFX
	3	**100.00**	0.20	**100.00**	0.85	**100.00**	1.02	101.00	0.18	DFX, SMR, M
4	0.1	159.00	46.12	127.00	42.41	**100.00**	27.06	136.50	51.62	M
	0.5	100.00	42.45	**87.00**	22.12	101.00	43.10	111.00	43.82	SMR
	1	79.00	8.45	**78.00**	5.00	82.00	22.13	79.00	5.96	SMR
	1.5	**75.00**	1.69	76.00	2.37	76.00	5.82	76.00	1.35	DFX
	2	**75.00**	0.53	**75.00**	1.28	75.00	0.90	76.00	0.48	DFX, SMR
	3	**75.00**	0.04	**75.00**	0.56	75.00	0.00	76.00	0.06	DFX, SMR
5	0.1	127.00	30.13	**107.00**	34.57	110.00	24.36	115.00	41.46	SMR
	0.5	80.00	29.38	**70.00**	17.43	88.00	31.31	82.00	30.76	SMR
	1	**62.00**	5.58	**62.00**	4.58	63.00	11.24	**62.00**	4.01	DFX, SMR, X
	1.5	**60.00**	1.03	61.00	1.90	**60.00**	1.46	61.00	1.01	DFX, M
	2	**60.00**	0.34	**60.00**	0.88	**60.00**	0.43	61.00	0.32	DFX, SMR, M
	3	**60.00**	0.00	**60.00**	0.36	**60.00**	0.00	61.00	0.11	DFx, SMR, M
8	0.1	**63.50**	17.67	73.50	19.48	67.00	19.33	75.00	25.51	DFX
	0.5	47.00	14.84	47.00	12.62	50.00	16.21	**46.00**	12.64	X
	1	**39.00**	1.59	40.00	3.73	**39.00**	2.41	**39.00**	1.44	DFX, M, X
	1.5	**38.00**	0.38	39.00	1.33	**38.00**	0.47	39.00	0.55	DFX, M
	2	**38.00**	0.08	**38.00**	0.64	**38.00**	0.13	**38.00**	0.50	DFX, SMR, M, X
	3	**38.00**	0.00	**38.00**	0.28	**38.00**	0.00	**38.00**	0.27	DFX, SMR, M, X
10	0.1	**52.00**	16.42	53.00	16.03	57.50	17.14	59.00	20.47	DFX
	0.5	37.00	10.68	47.00	13.48	39.50	11.99	**35.00**	8.54	X
	1	**30.00**	1.06	40.00	12.26	**30.00**	1.31	31.00	0.92	DFX, M
	1.5	**30.00**	0.25	34.00	7.69	**30.00**	0.30	31.00	0.18	DFX, M
	2	**30.00**	0.00	32.00	4.04	**30.00**	0.04	31.00	0.10	DFX, M
	3	**30.00**	0.00	31.00	1.95	**30.00**	0.00	31.00	0.04	DFX, M

Nominal ARL_0 is set to ~370 ($\alpha = 0.0027$ resulting $k = 3$).
[a] M = Median, SMR = Standardized Mean-Rank, DFX = DF X-bar, X = X-bar.

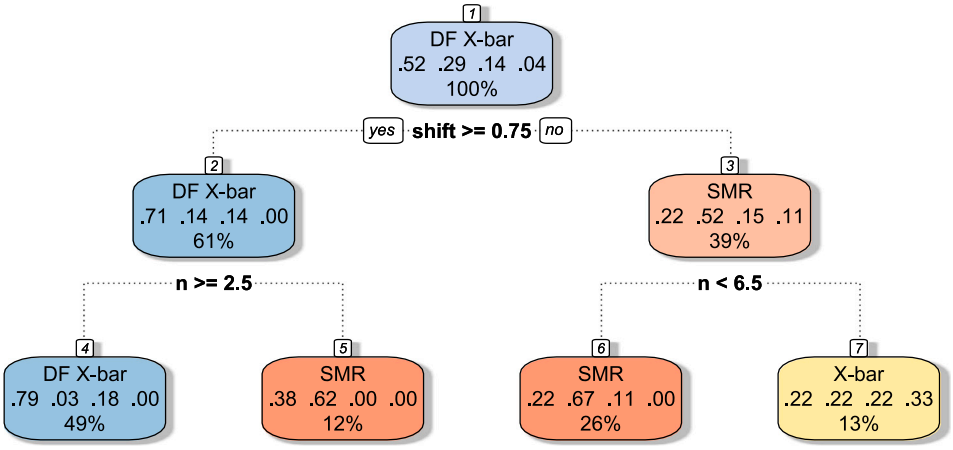


Fig. 12. Control chart recommendations for an OP, aiming to minimize ARL_1.

Fig. 12 supports practitioners in the control chart selection since it shows the preferred control charts on the basis of the desired sample size and expected shift size. Each leaf of the decision tree denotes the best control chart according to the combination of the input parameters (n, z). The classification trees define the cutoff points that provide the purest classes as much as possible. To measure purity, the Gini index and entropy are measured for each split (Ferreira and Vasilyev, 2015). With this strategy, the cutoff point for the shift size is 0.75. If $z > 0.75$ and at least $n = 3$ samples can be taken, the DF X-bar chart provides the best performance. If the shift size remains the same but n must be smaller because the process is long and it takes a long time to collect samples with high n, the SMR chart is recommended to obtain the lowest ARL_1. When $z \leq 0.75$ and $n < 7$, the SMR chart still has the best performance. In this small-shift scenario with a greater sample size ($n > 7$), the Shewhart X-bar chart can be used. Notably, the median chart is not shown in the decision tree in any of these cases since it

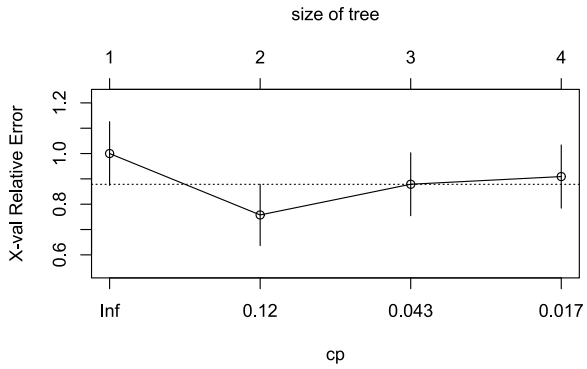


Fig. 13. Control chart recommendations for an OP, aiming to minimize ARL_1.

performs better than the other control charts in very few special cases. Therefore, the ratio of cases where the median chart outperforms the others is negligible during the formulation of the overall control chart selection rules. A further notable observation based on the decision tree results is that in control chart selection, the shift size has greater importance than the sample size since the shift size takes a higher level in the tree hierarchy (splitting is performed starting with the independent variable that has the strongest influence on the dependent variable). This observation also suggests that in control chart selection for OPs, the shift size should be considered first. The data in Fig. 12 confirm the observations in Fig. 11.

In this study, the independence of the TPT values was assumed, and this assumption was supported by the absence of significant autocorrelation among the data points. However, autocorrelation could appear in OP data in several cases; in this situation, autoregressive integrated moving average (ARIMA) control charts can be used (Costa and Fichera, 2021; Yao et al., 2023) even if the collected data are also subject to measurement uncertainty (Sabahno, 2023).

4.2.1. *Sensitivity analysis for distribution types*

The control chart performance is also analyzed when different distribution types are assumed. During the simulation, the initial distribution parameters were used, and the 3rd and 4th moments of the distribution, i.e., skewness and kurtosis, were changed stepwise to generate TPT observations. Afterward, the same ARL_1 calculation was conducted, as described in Section 4.2. The 14 values in each chart for different combinations of skewness and kurtosis are shown in Figure ARL_1. Tests were performed under different sample sizes and shift assumptions (left side of Fig. 14). In each contour subfigure, the color reflects the ARL_1 value for the given combination of skewness (x-axis) and kurtosis (y-axis).

Overall, the results show that the analyzed control charts are insensitive to the distribution type since the ARL_1 change is approximately 1–2 on average (see the color bars), even with a smaller sample size (n = 5). The X-bar chart is the only exception, but this sensitivity also weakens if the sample size and shift size increase, which is expected because of the effect of the central limit theorem. Interestingly, the median and DF X-bar charts differ when n = 5. While X-bar and SMR charts have higher ARL_1 values for symmetric distributions, the other two charts increase at extreme values for skewness and kurtosis;

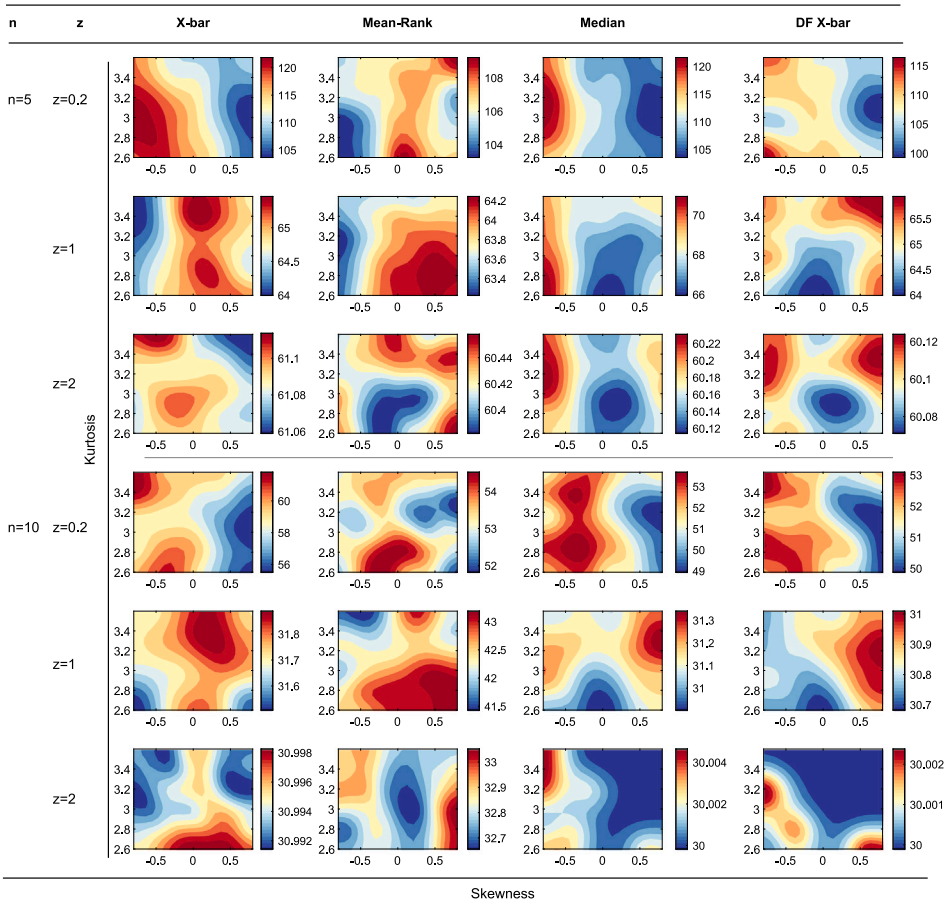


Fig. 14. Control chart recommendations for an OP, aiming to minimize ARL_1. (For interpretation of the references to color in this figure legend, the reader is referred to the web version of this article.)

however, this change is still insignificant, and when $n = 10$ and $z = 2$, these control charts have very small reactions to any change in the distribution parameters. This analysis also confirms that the selected control charts are good choices for monitoring OPs since they are robust to changes in the distribution parameters.

5. Summary and conclusion

In this paper, we proposed a control chart for monitoring and controlling OPs (C_1). The structure of the proposed control chart and the chart selection and design process are also given (C_2). The proposed method was tested on a real OP example and on simulations. The OP chart proved to be applicable to real-life and simulated OPs (C_3). The results showed that the sample size and shift size significantly affect the performance of the control charts. The analyzed distribution-free control charts are an excellent solution for OP monitoring when normality cannot be guaranteed. As a further contribution, this paper provides a recommendation scheme for the analyzed control charts for OPs to achieve better out-of-control performance (C_4). The implications of this paper can help practitioners control OPs and support decision-making for OP chart selection (C_5).

In future work, benchmarking the OP chart against advanced SPC methods such as cumulative sum chart (CUSUM) and exponentially weighted moving average control chart (EWMA) under complex, mixed-distribution scenarios from EPC subprocesses could be a potential direction. Such comparisons would reveal its sensitivity to subtle shifts and robustness across diverse data patterns, thereby underscoring its value for real-world applications.

CRediT authorship contribution statement

Zsolt T. Kosztyán: Writing – review & editing, Writing – original draft, Visualization, Supervision, Methodology, Formal analysis, Data curation, Conceptualization. **Andrew MacClever:** Writing – review & editing, Writing – original draft, Data curation, Visualization, Resources, Data curation. **Zahid Khan:** Writing – review & editing, Formal analysis, Data curation. **Csaba Hegedűs:** Writing – review & editing, Writing – original draft, Visualization, Methodology, Data curation, Conceptualization. **Aamir Saghir:** Methodology, Data curation. **Tibor Csizmadia:** Writing – review & editing, Writing – original draft, Validation, Data curation. **Attila I. Katona:** Writing – review & editing, Writing – original draft, Visualization, Validation, Methodology, Formal analysis, Data curation, Conceptualization.

Funding

This work has been implemented by the TKP2021-NVA-10 project, with support provided by the Ministry of Culture and Innovation of Hungary from the National Research, Development and Innovation Fund, financed under the 2021 Thematic Excellence Programme funding scheme.

Declaration of competing interest

The authors declare that they have no known competing financial interests or personal relationships that could have appeared to influence the work reported in this paper.

Appendix A. List of abbreviations

Glossary

ARIMA Autoregressive integrated moving average

BPMN Business process model and notation

CUSUM Cumulative sum chart

DFD Data flow diagram

EPC Event-driven process chain

ERP Enterprise resource planning

EWMA Exponentially weighted moving average control chart

FAP False alarm probability

MES Manufacturing execution system

OP Operation process

SMR Standardized mean–rank

SPC Statistical process control

TPC Total process cost

TPT Total process time

UML Unified modeling language

VSM Value stream mapping

Appendix B. Detailed task descriptions related to the maintenance process

See Table B.11.

Appendix C. Other examples for real-world applications: Human resource recruitment process

Although the usage of the proposed methods is independent of OP, in this section, the application of control charts for operation processes is demonstrated in a more general real-world business process, the recruitment and selection of white-collar human resources, which is performed similarly in several industries. The examined process (see the EPC in Fig. C.15) has 30 tasks with 3 decision points, such as *'Choosing the recruitment methods and cohorts'* ($T9$) and then *'Choosing internal succession and replacement plans'* ($T10$) or *'Selection of external recruitment methods and channels'* ($T14$), and several parallel task executions. The whole process starts with *'Identifying a gap between needed and available human resources'* and ends with *'Selecting the most suitable applicant (to eliminate the discrepancy)'*. None of the 30 tasks have normally distributed durations, and since costs depend mostly on the amount of time spent working, costs also do not follow a normal distribution.

All 30 tasks of the recruitment process are listed in Table C.12.

The taskwise distributions of the standardized durations are shown in Fig. C.16.

Similar to the maintenance process, the normality if not fulfilled by the taskwise distributions in this example is also confirmed by Fig. C.16. The fitted control charts for monitoring the overall process C.17 are shown in Fig. TPT. During chart fitting, 50 samples were collected, and the sample size was chosen as $n = 2$. The reason behind this choice is also technical in this case, since the opportunity for data collection is infrequent (compared with the maintenance process) in this case, and a small sample size is preferred to ensure an adequate number of sample points during the control.

As the chart patterns and control line positions suggest, the SMR chart is a good candidate for early detection of process shifts because it has the narrowest control interval. To analyze the more detailed control chart behavior under different shift sizes, the same simulation is conducted as presented in Section 4.2. The parameter setting is also

Table B.11
Description of each task in the operational process.

Task	Description
t_1	Production is stopped.
t_2	Maintenance personnel are called to inspect the machine.
t_3	The cause of the error is determined.
t_4	The production manager notifies the management.
t_5	The management assigns the task to the procurement manager.
t_6	It is ascertained whether the machine is under warranty.
t_7	A price quote is requested from the machine's manufacturing company by procurement.
t_8	The request for a price quote is received by the manufacturing company.
t_9	Experts from the manufacturing company are sent to the company to assess the nature of the error.
t_{10}	Following the assessment, the findings are summarized, and a price quote for the repair costs is sent.
t_{11}	Procurement informs the company's management regarding the price quote.
t_{12}	A decision is made concerning the price quote.
t_{13}	The price quote is negotiated with the supplier.
t_{14}	The price quote is accepted.
t_{15}	The manufacturing company is notified of the acceptance of the price quote, and the contract is concluded.
t_{16}	The manufacturing company commences the execution of the assignment.
t_{17}	The malfunctioning machine is transported to the manufacturing company.
t_{18}	The repair of the machine and the replacement of parts are initiated by the experts.
t_{19}	Trial production is conducted on the repaired machine.
t_{20}	Quality is checked by the responsible inspector.
t_{21}	The cause of the error is examined.
t_{22}	The product is manufactured again.
t_{23}	The repaired machine is transported to the production company.
t_{24}	The faulty machine is returned to the company providing the warranty.
t_{25}	The new machine is returned by the suppliers.
t_{26}	The machine is taken into the company's inventory.
t_{27}	Procurement is notified about it.
t_{28}	Procurement informs the warehouse staff and maintenance personnel.
t_{29}	The machine is repaired on-site by the experts.
t_{30}	The machine is put into operation.
t_{31}	Trial production is performed on the machine.
t_{32}	The machine is put back into production.
t_{33}	The fulfillment of orders is resumed.
t_{34}	The rectification of the error is checked by management.
t_{35}	The invoice is paid.
t_{36}	Production returns to its state prior to the error.

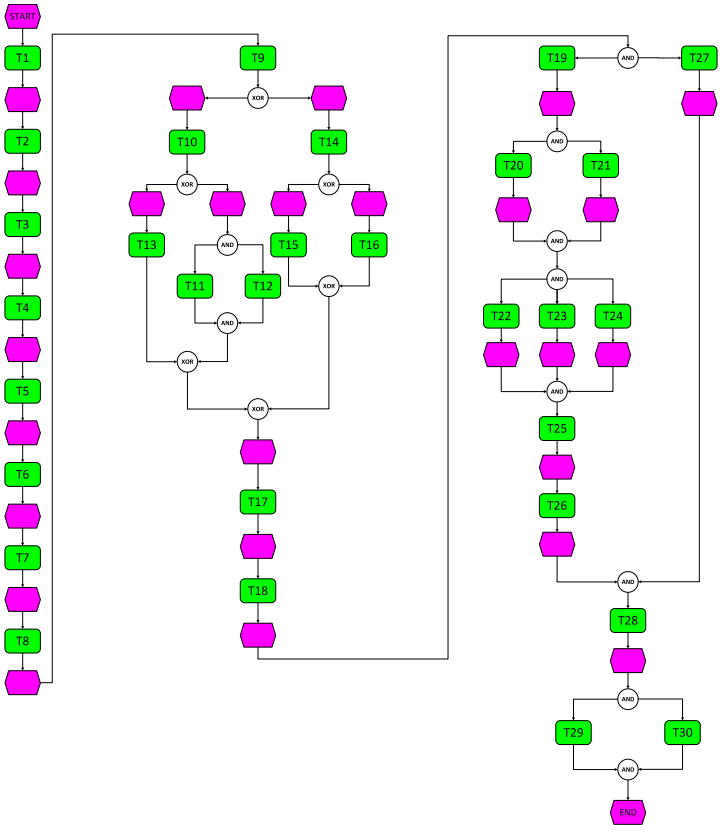


Fig. C.15. EPC model of the recruitment process in the case of organizational change.

Table C.12
Description of each task in the recruitment process.

Task	Description
T1	Identifying a gap between needed and available human resources
T2	Labor demand is assessed
T3	Analysis of labor utilization
T4	Labor requirement calculation
T5	Decision about required headcount and initiation of requirement process
T6	Analysis of the job specifications for a given position
T7	Job descriptions are compiled based on job specifications
T8	Preparing for recruitment, listing applicable methods
T9	Choosing the recruitment methods and cohorts
T10	Choosing internal succession and replacement plans
T11	Consultation with all managers concerned
T12	Consultation with employees (candidates/affected parties)
T13	Development of required plans
T14	Selection of external recruitment methods and channels
T15	Establishing contact with the appropriate entities
T16	Development of the background for external recruitment and the necessary tools
T17	Creating job advertisements based on the job descriptions
T18	Posting the advertisements and sending them for publishing
T19	First filtering of candidates
T20	Suitable candidates are invited for an interview
T21	Unsuitable candidates are informed of their unsuccessful application
T22	Booking a meeting room
T23	Informing the reception about the arrival of new people
T24	Preparing an interview schedule
T25	Arrival and reception of interviewees
T26	Interviewing
T27	The HR department receives and administers CVs
T28	Selecting the most suitable applicant (to eliminate the discrepancy)
T29	Notification of rejected candidates
T30	Notification of selected candidate



Fig. C.16. Distribution of standardized durations for each task in the recruitment process.

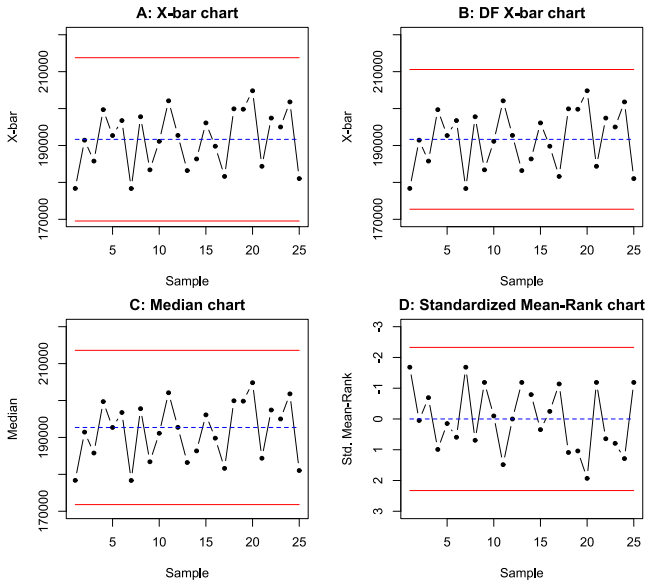


Fig. C.17. Control charts fitted for the recruitment process considering TPT as the control variable.

Table C.13
Control chart performances on the human resource recruitment process ($n = 2$).

Metric	z	Chart				Best chart[a]
		DF X-bar	SMR	Median	X-bar	
ARL_1	0.5	92.21	**27.91**	124.74	129.80	SMR
	1	52.51	**6.55**	79.69	87.85	SMR
	1.5	6.20	**3.68**	38.00	7.99	SMR
	2	**2.44**	2.58	8.99	4.71	DFX
	3	**1.18**	1.95	5.62	2.34	DFX
MRL_1	0.5	22.00	**13.00**	22.00	42.00	SMR
	1	12.00	**4.50**	9.00	17.00	SMR
	1.5	**3.00**	**3.00**	5.00	4.00	SMR/DFX
	2	**1.50**	2.00	2.00	3.00	DFX
	3	**1.00**	**1.00**	**1.00**	2.00	SMR/DFX/M
$SDRL_1$	0.5	167.53	**45.81**	211.96	216.32	SMR
	1	125.19	**7.37**	214.35	197.74	SMR
	1.5	10.27	**3.00**	116.15	11.07	SMR
	2	2.88	**1.93**	18.26	5.23	SMR
	3	**0.58**	1.55	24.20	0.71	DFX

Nominal ARL_0 is set to ~370 ($\alpha = 0.0027$ resulting $k = 3$).
[a] M = Median, SMR = Standardized Mean-Rank, DFX = DF X-bar, X = X-bar.

the same as that presented in Table 9. Table C.13 shows the results of the simulation.

As Table C.13 shows, the SMR chart is suggested for use when $z < 2$; otherwise, the DF X-bar chart is the adequate choice. As the results for this practical example show, distribution-free control charts are preferred for use in each case compared with the X-bar chart.

Data availability

The analyzed maintenance process data are freely available on the Figshare platform (Kosztyán et al., 2025).

References

Abbas, Z., Nazir, H.Z., Abid, M., Akhtar, N., Riaz, M., 2021. Nonparametric progressive sign chart for monitoring process location based on individual data. Qual. Technol. Quant. Manag. 18 (2), 225–247. http://dx.doi.org/10.1080/16843703.2020.1827726.

Abbas, Z., Nazir, H.Z., Riaz, M., Abid, M., Akhtar, N., 2023. An efficient nonparametric double progressive mean chart for monitoring of the process location. Comm. Statist. Simulation Comput. 52 (6), 2578–2591.

Abbas, Z., Nazir, H.Z., Xiang, D., Shi, J., 2024. Nonparametric adaptive cumulative sum charting scheme for monitoring process location. Qual. Reliab. Eng. Int..

Abid, M., Nazir, H.Z., Riaz, M., Lin, Z., 2017. An efficient nonparametric EWMA Wilcoxon signed-rank chart for monitoring location. Qual. Reliab. Eng. Int. 33 (3), 669–685.

Adekeye, K.S., Adewara, J.A., Aako, O.L., Olaomi, J.O., 2021. Performance of median absolute deviation and some alternatives to median absolute deviation control charts for skewed and heavily tailed process. Qual. Reliab. Eng. Int. 37 (8), 3431–3440. http://dx.doi.org/10.1002/qre.2926.

Ahmadini, A.A., Abbas, T., AlQadi, H., 2025. Adaptive EWMA control chart by adjusting the risk factors through artificial neural network. Qual. Reliab. Eng. Int. 41 (3), 992–1001.

Ahmed, F., Mahmood, T., Riaz, M., Abbas, N., 2024. Comprehensive review of high-dimensional monitoring methods: trends, insights, and interconnections. Qual. Technol. Quant. Manag. 1–25.

Albers, W., Kallenberg, W.C., Nurdiati, S., 2004. Parametric control charts. J. Statist. Plann. Inference 124 (1), 159–184.

Alevizakos, V., Chatterjee, K., Koukouvinos, C., 2024. Distribution-free Phase II triple EWMA control chart for joint monitoring the process location and scale parameters. J. Appl. Stat. 51 (6), 1171–1190.

Almazah, M.M.A., Ali, F.A.M., Eltayeb, M.M., Atta, A., 2021. Comparative analysis four different ways of calculating yield index SSS pk based on information of control chart, and six sigma, to measuring the process performance in industries: Case study in Aden's Oil Refinery, Yemen. IEEE Access 9, 134005–134021.

Amjad, A., Azam, F., Anwar, M.W., Butt, W.H., Rashid, M., 2018. Event-driven process chain for modeling and verification of business requirements–a systematic literature review. IEEE Access 6, 9027–9048. http://dx.doi.org/10.1109/ACCESS.2018.2791666.

Bakir, S.T., 2004. A distribution-free Shewhart quality control chart based on signed-ranks. Qual. Eng. 16 (4), 613–623. http://dx.doi.org/10.1081/QEN-120038022.

Bi, H.H., 2022. Applying statistical process control to teaching quality assurance at higher education institutions. Qual. Manag. J. 29 (2), 145–157. http://dx.doi.org/10.1080/10686967.2022.2035288.

Caivano, D., 2005. Continuous software process improvement through statistical process control. In: Ninth European Conference on Software Maintenance and Reengineering. IEEE, pp. 288–293. http://dx.doi.org/10.1109/CSMR.2005.20.

Capizzi, G., Masarotto, G., 2018. Phase I distribution-free analysis with the R package dfphase1. In: Frontiers in Statistical Quality Control 12. Springer, pp. 3–19.

Castagliola, P., Achouri, A., Taleb, H., Celano, G., Psarakis, S., 2013. Monitoring the coefficient of variation using control charts with run rules. Qual. Technol. Quant. Manag. 10 (1), 75–94.

Castagliola, P., Figueiredo, F.O., 2013. The median chart with estimated parameters. Eur. J. Ind. Eng. 7 (5), 594–614. http://dx.doi.org/10.1504/EJIE.2013.057382.

Chakraborti, S., Graham, M.A., 2019. Nonparametric (distribution-free) control charts: An updated overview and some results. Qual. Eng. 31 (4), 523–544. http://dx.doi.org/10.1080/08982112.2018.1549330.

Chakraborti, S., Van der Laan, P., Bakir, S., 2001. Nonparametric control charts: an overview and some results. J. Qual. Technol. 33 (3), 304–315. http://dx.doi.org/10.1080/00224065.2001.11980081.

Chen, X., Mukherjee, A., Xiang, D., Li, W., 2025. A phase-II change-point-based distribution-free scheme for monitoring of three process aspects. J. Nonparametr. Stat. 37 (1), 128–147.

Chowdhury, S., Mukherjee, A., Chakraborti, S., 2014. A new distribution-free control chart for joint monitoring of unknown location and scale parameters of continuous distributions. Qual. Reliab. Eng. Int. 30 (2), 191–204.

Colin, J., Vanhoucke, M., 2015. Developing a framework for statistical process control approaches in project management. Int. J. Proj. Manage. 33 (6), 1289–1300. http://dx.doi.org/10.1016/j.ijproman.2015.03.014.

Costa, A., Fichera, S., 2021. Economic-statistical design of adaptive arma control chart for autocorrelated data. J. Stat. Comput. Simul. 91 (3), 623–647. http://dx.doi.org/10.1080/00949655.2020.1825716.

Das, K.R., Imon, A., 2016. A brief review of tests for normality. Am. J. Theor. Appl. Stat. 5 (1), 5–12.

Davis, R.B., Woodall, W.H., 1988. Performance of the control chart trend rule under linear shift. J. Qual. Technol. 20 (4), 260–262. http://dx.doi.org/10.1080/00224065.1988.11979118.

Diaz Pulido, A.J., Cordero Franco, A.E., Tercero Gómez, V.G., 2023. A distribution-free control chart for joint monitoring of location and scale in finite horizon productions. Comput. Statist. 1–19.

Diaz Pulido, A.J., Cordero Franco, A.E., Tercero Gómez, V.G., 2025. A distribution-free control chart for joint monitoring of location and scale in finite horizon productions. Comput. Statist. 40 (6).

Dijkman, R., Hofstetter, J., Koehler, J., 2011. Business Process Model and Notation, vol. 89, Springer, http://dx.doi.org/10.1007/978-3-642-25160-3.

Ferreira, D.R., Vasilyev, E., 2015. Using logical decision trees to discover the cause of process delays from event logs. Comput. Ind. 70, 194–207.

Godase, D.G., Mahadik, S.B., 2024. The combined Shewhart-CUSUM sign charts. Comm. Statist. Simulation Comput. 53 (1), 357–366.
Goedhart, R., Schoonhoven, M., Does, R.J., 2017. Guaranteed in-control performance for the Shewhart X and X control charts. J. Qual. Technol. 49 (2), 155–171.
Graham, M., Human, S., Chakraborti, S., 2010. A Phase I nonparametric Shewhart-type control chart based on the median. J. Appl. Stat. 37 (11), 1795–1813.
Hajej, Z., Nyoungue, A.C., Abubakar, A.S., Mohamed Ali, K., 2021. An integrated model of production, maintenance, and quality control with statistical process control chart of a supply chain. Appl. Sci. 11 (9), 4192. http://dx.doi.org/10.3390/app11094192.
Hillier, F.S., 1967. Small sample probability limits for the range chart. J. Amer. Statist. Assoc. 62 (320), 1488–1493.
Ikpotokin, O., Ishiekwene, C., 2016. Permutation approach in obtaining control limits and interpretation of out of control signals in multivariate control charts. Int. J. Stat. Appl. 6 (6), 408–415.
ISO Central Secretary, 2023. Control Charts – Part 2 Shewhart Control Charts. Standard ISO 7870-2:2023(E), 2023, International Organization for Standardization, Geneva, CH.
Jayathavaj, V., Pongpullponsak, A., 2014. A simulation study on the performance of the sign test, Mann-Whitney test, Hodges-Lehmann estimator and control charts for Normal and Weibull data. Int. J. Ind. Eng. Comput. 5 (4), 561–574.
Jones-Farmer, L.A., Jordan, V., Champ, C.W., 2009. Distribution-free phase I control charts for subgroup location. J. Qual. Technol. 41 (3), 304–316.
Katona, A., 2022. Validation of risk-based quality control techniques: a case study from the automotive industry. J. Appl. Stat. 49 (12), 3236–3255. http://dx.doi.org/10.1080/02664763.2021.1936466.
Khorshidi, H.A., Nikfalazar, S., Gunawan, I., 2016. Statistical process control application on service quality using SERVQUAL and QFD with a case study in trains' services. TQM J. 28 (2), 195–215.
Kim, J., Lim, C., 2021. Customer complaints monitoring with customer review data analytics: An integrated method of sentiment and statistical process control analyses. Adv. Eng. Informatics 49, 101304. http://dx.doi.org/10.1016/j.aei.2021.101304.
Klein, M., 2000. Two alternatives to the Shewhart X control chart. J. Qual. Technol. 32 (4), 427–431. http://dx.doi.org/10.1080/00224065.2000.11980028.
Knoth, S., 2021. Controlling the exponentially weighted moving average S 2 control chart false alarm behavior when the in-control variance level must be estimated. Appl. Stoch. Models Bus. Ind. 37 (4), 725–743. http://dx.doi.org/10.1002/asmb.2613.
Kostyszyn, K.N., Brandstätter, T.C., Vollmer, T., Schmitt, R., 2021. Statistical testing for sufficient control chart performances during monitoring of grouped processes. Qual. Reliab. Eng. Int. 37 (6), 2555–2567. http://dx.doi.org/10.1002/qre.2875.
Kosztyán, Z.T., Katona, A.I., 2016. Risk-based multivariate control chart. Expert Syst. Appl. 62, 250–262. http://dx.doi.org/10.1016/j.eswa.2016.06.019.
Kosztyán, Z.T., Katona, A.I., 2018. Risk-based X-bar chart with variable sample size and sampling interval. Comput. Ind. Eng. 120, 308–319. http://dx.doi.org/10.1016/j.cie.2018.04.052.
Kosztyán, Z.T., MacClever, A.B., Khan, Z., Hegedűs, C., Csizmadia, T., Katona, A., 2025. Application of statistical control charts for operation processes. http://dx.doi.org/10.6084/m9.figshare.c.7816277.v1, URL: https://figshare.com/collections/Application_of_statistical_control_charts_for_operation_processes/7816277/1.
Koutras, M., Bersimis, S., Maravelakis, P., 2007. Statistical process control using Shewhart control charts with supplementary runs rules. Methodol. Comput. Appl. Probab. 9, 207–224. http://dx.doi.org/10.1007/s11009-007-9016-8.
Lasa, I.S., Laburu, C.O., de Castro Vila, R., 2008. An evaluation of the value stream mapping tool. Bus. Process. Manag. J. 14 (1), 39–52. http://dx.doi.org/10.1108/14637150810849391.
Li, Q., Chen, Y.-L., 2009. Data flow diagram. In: Modeling and Analysis of Enterprise and Information Systems. Springer, pp. 85–97. http://dx.doi.org/10.1007/978-3-540-89556-5_4.
Li, Y., Pei, D., Wu, Z., 2020. A multivariate non-parametric control chart based on run test. Comput. Ind. Eng. 149, 106839.
Li, Z., Xie, M., Zhou, M., 2018. Rank-based EWMA procedure for sequentially detecting changes of process location and variability. Qual. Technol. Quant. Manag. 15 (3), 354–373. http://dx.doi.org/10.1080/16843703.2016.1208941.
Mastrangelo, C.M., Brown, E.C., 2000. Shift detection properties of moving centerline control chart schemes. J. Qual. Technol. 32 (1), 67–74. http://dx.doi.org/10.1080/00224065.2000.11979972.
Mukherjee, A., Chakraborti, S., 2012. A distribution-free control chart for the joint monitoring of location and scale. Qual. Reliab. Eng. Int. 28 (3), 335–352.
Mukherjee, A., Sen, R., 2015. Comparisons of Shewhart-type rank based control charts for monitoring location parameters of univariate processes. Int. J. Prod. Res. 53 (14), 4414–4445.
Muñoz, J.J., Aslam, M., Campuzano, M.J., 2023. Optimized repetitive sampling X-bar control chart: performance evaluation and comparison with Shewhart control chart. Front. Appl. Math. Stat. 9, 1285023.
Myles, A.J., Feudale, R.N., Liu, Y., Woody, N.A., Brown, S.D., 2004. An introduction to decision tree modeling. J. Chemom.: A J. Chemom. Soc. 18 (6), 275–285.
Oakland, J., Oakland, R.J., 2018. Statistical Process Control. Routledge.
Perdikis, T., Celano, G., Chakraborti, S., 2024. Distribution-free control charts for monitoring scale in finite horizon productions. European J. Oper. Res. 314 (3), 1040–1051.
Qiu, P., Li, Z., 2011. On nonparametric statistical process control of univariate processes. Technometrics 53 (4), 390–405.
Qiu, P., Li, W., Li, J., 2020. A new process control chart for monitoring short-range serially correlated data. Technometrics 62 (1), 71–83. http://dx.doi.org/10.1080/00401706.2018.1562988.
Ruiz-Tamayo, J., Vazquez-Lopez, J.A., Ruelas-Santoyo, E.A., Hernandez-Lopez, A., Lopez-Juarez, I., Rios-Lira, A.J., 2021. Multivariate pattern recognition in MSPC using Bayesian inference. Mathematics 9 (4), 306. http://dx.doi.org/10.3390/math9040306.
Sabahno, H., 2023. An adaptive max-type multivariate control chart by considering measurement errors and autocorrelation. J. Stat. Comput. Simul. 93 (16), 2956–2981. http://dx.doi.org/10.1080/00949655.2023.2214830.
Sabahno, H., Amiri, A., 2023. New statistical and machine learning based control charts with variable parameters for monitoring generalized linear model profiles. Comput. Ind. Eng. 184, 109562.
Scheer, A.-W., Kruppke, H., Jost, W., Kindermann, H., 2006. Agility by ARIS Business Process Management: Yearbook Business Process Excellence 2006/2007, vol. 243, Springer Science & Business Media.
Schilling, E.G., Nelson, P.R., 1976. The effect of non-normality on the control limits of X charts. J. Qual. Technol. 8 (4), 183–188. http://dx.doi.org/10.1080/00224065.1976.11980743.
Severin, T., Schmid, W., 1998. Statistical process control and its application in finance. In: Risk Measurement, Econometrics and Neural Networks: Selected Articles of the 6th Econometric-Workshop in Karlsruhe, Germany. Springer, pp. 83–104. http://dx.doi.org/10.1007/978-3-642-58272-1_7.
Shi, L., Sun, Y., He, Y., He, Z., 2025. Bi-channel dynamic topic model for quality monitoring considering initial and additional online customer reviews. IISE Trans. 57 (11), 1277–1294.
Siau, K., Cao, Q., 2001. Unified modeling language: A complexity analysis. J. Database Manag. (JDM) 12 (1), 26–34. http://dx.doi.org/10.4018/jdm.2001010103.
Teoh, W.L., Khoo, M.B., Castagliola, P., Yeong, W.C., Teh, S.Y., 2017. Run-sum control charts for monitoring the coefficient of variation. European J. Oper. Res. 257 (1), 144–158.
Thor, J., Lundberg, J., Ask, J., Olsson, J., Carli, C., Härenstam, K.P., Brommels, M., 2007. Application of statistical process control in healthcare improvement: systematic review. BMJ Qual. Saf. 16 (5), 387–399. http://dx.doi.org/10.1136/qshc.2006.022194.
Toma, H.M., Abdelazim, A.N., Ibrahim, A.H., 2025. Assessment of estimation performance for activities' cost and time in construction projects using statistical process control. Eng. Constr. Archit. Manag..
Tran, P.H., Tran, K.P., Rakitzis, A., 2019. A synthetic median control chart for monitoring the process mean with measurement errors. Qual. Reliab. Eng. Int. 35 (4), 1100–1116.
Wang, Z., Wu, Q., Qiu, P., 2024. Novel nonparametric control charts for monitoring dispersion of count data. Qual. Reliab. Eng. Int. 40 (4), 1636–1651.
Waqas, M., Xu, S.H., Anwar, S.M., Rasheed, Z., Masengo, G., 2025. An enhanced EWMA model for statistical insights in process monitoring with application in brake pad failure and carbon fiber strength. J. Stat. Theory Appl. 1–31.
Waqas, M., Xu, S.H., Anwar, S.M., Rasheed, Z., Shabbir, J., 2023. The optimal control chart selection for monitoring COVID-19 phases: a case study of daily deaths in the USA. Int. J. Qual. Health Care 35 (3), mzad058. http://dx.doi.org/10.1093/intqhc/mzad058.
Williams, B., Ziemnik, L., 2025. Selecting the correct control chart: A practical example from adolescent care. Curr. Probl. Pediatr. Adolesc. Health Care 55 (7), 101805.
Wu, C., Zhao, Y., Wang, Z., 2002. The median absolute deviations and their applications to Shewhart control charts. Comm. Statist. Simulation Comput. 31 (3), 425–442. http://dx.doi.org/10.1081/SAC-120003850.
Xue, L., Wang, Q., He, Z., Qiu, P., 2024. A nonparametric EWMA control chart for monitoring mixed continuous and count data. Qual. Technol. Quant. Manag. 21 (5), 749–765. http://dx.doi.org/10.1080/16843703.2023.2246765.
Yang, S.-F., Lin, J.-S., Cheng, S.W., 2011. A new nonparametric EWMA sign control chart. Expert Syst. Appl. 38 (5), 6239–6243.
Yao, Y., Chakraborti, S., Yang, X., Parton, J., Lewis, D., Hudnall, M., 2023. Phase I control chart for individual autocorrelated data: application to prescription opioid monitoring. J. Qual. Technol. 55 (3), 302–317. http://dx.doi.org/10.1080/00224065.2022.2139783.
Zhong, J., Jia, F., 2025. Supply chain risk transmission monitoring based on graphic evaluation and review technique. Heliyon 11 (1).
Zhou, W., Liu, N., Zheng, Z., 2020. A synthetic control chart for monitoring the small shifts in a process mean based on an attribute inspection. Comm. Statist. Theory Methods 49 (9), 2189–2204. http://dx.doi.org/10.1080/03610926.2019.1568491.
Zhou, Q., Luo, Y., Wang, Z., 2010. A control chart based on likelihood ratio test for detecting patterned mean and variance shifts. Comput. Statist. Data Anal. 54 (6), 1634–1645.